Radio Wave Propagation in Metal Train Compartments

logica

TU Delft

Yaowen Khee

January 12, 2009

Radio Wave Propagation in Metal Train Compartments

MSc thesis in Embedded Systems

Faculty of Electrical Engineering, Mathematics, and Computer Science
Delft University of Technology
The Netherlands

Yaowen Khee

January 12, 2009

Author
Yaowen Khee yb.khee@gmail.com

Title
Radio Wave Propagation in Metal Train Compartments

Credit Points
40 EC

Presentation Date
January 23, 2009

Graduation Committee

prof. dr. K.G. Langendoen (chair)	Delft University of Technology
dr. ir. A.J. van Genderen	Delft University of Technology
ir. E.C. Essenius	Logica B.V.
drs. B. Vranken	Logica B.V.
dr. ing. P.J.M. Havinga	University of Twente

Abstract

Wireless sensor networks are being deployed extensively to collect sensory data in various environments under different conditions. A wireless sensor network consists of multiple nodes, each with the ability to communicate using radio waves. The characteristics of the radio link between nodes are largely influenced by their environment. For instance, a radio link between two nodes with obstructed line-of-sight behaves more erratic than one that is not obstructed.

This thesis focuses primarily on the characteristics of radio wave propagation in metal train compartments from a Computer Science standpoint. It means that the electrical aspects of this subject are not discussed in detail. In this work, we focus mainly on matters such as transmission output power, signal strength, preamble length, and packet reception rate.

Various tests were performed throughout the length of the project. The purpose of the tests was to gain insights on the characteristics of radio wave propagation under various circumstances. We examine the effect exerted on radio wave propagation by varying transmission output power, antenna orientation, and antenna position. The characteristics reported in this thesis are signal strength, preamble length, and packet reception rate. The tests were carried out in an open field and in metal train compartments. The open field tests were used to create benchmark data for which data from metal train compartments could be compared with.

The tests have led to several important findings. They show that radio links could be established within metal train compartments and even between two compartments. The latter seems to contradict rational belief that radio waves cannot propagate from one train compartment to the other, because of the metallic structure. Furthermore, there are some indications that antenna orientation may greatly influence radio wave propagations in compartments for low transmission output powers. This thesis also examines the preamble length. It finds that the preamble length could potentially be reduced to two bytes without affecting packet reception rates. And finally, the results show that higher transmission output power leads to greater packet reception rates and stronger received signal strengths, regardless of the environment. These and other findings are discussed in detail in the remainder of this thesis.

Acknowledgement

This thesis was made possible by Logica B.V., which provided most of the needed facilities. Bram Vranken, Edwin Essenius, and Cerion Armour-Brown were incredibly helpful on behalf of Logica B.V. Academic expertise was provided by Professor dr. Koen Langendoen, who gave excellent feedback and guidance. I express my gratitude to Venkatraman Iyer for lending me a hand in some key measurements and for having to suffer in the freezing mud. Lulu Fan has been very helpful in creating the cover page for this work. I am especially grateful to Winelis Kavelaars of SOWNet for providing the hardware. I am also very grateful to Kees van Broekhoven and Jeroen Davids of NedTrain for providing the trains. Finally, I wish to thank my family, friends, and colleagues for their everlasting support.

Contents

1 Introduction

Wireless sensor networks (WSNs) have become a valuable tool for researchers to collect sensory data. A WSN consists of autonomous sensor nodes. A node has the ability to communicate wirelessly with other nodes. Their popularity is contributed to their flexibility and ease of deployment. WSNs do not need fixed infrastructure and existing infrastructure may remain undisturbed. However, users should take into account the energy consumption and the environment of such networks. The operational lifespan of WSNs is directly dependent on energy consumption, as energy is nearly always supplied through batteries. The environment is also crucial, because it can be a limiting factor in positioning individual nodes. Obstruction in the path of radio waves may cause interference in radio communication. All these issues must be addressed in order to achieve a functional network.

This work is part of a larger research commissioned by Logica B.V. The research is to provide insights on how WSNs can be deployed to serve the needs of train passengers. This thesis in particular explores the radio wave propagation characteristics of WSNs within metal train compartments from a Computer Science standpoint, meaning that the electrical aspects are not discussed in detail. Results of this thesis will shed some light on whether it is possible to deploy this technology in this environment.

It is assumed that metal train compartments are a challenging environment for any kind of WSN application. Conducting materials, like the outer haul of train compartments, are known to reflect radio energy instead of letting it through. During the course of the project, very little data was found on WSN deployments in metallic environments. This led to the belief that deployment of WSNs in such an environment is impractical. However, a short online article (Kevan, 2006) claims the successful usage of a WSN inside the engine room of a ship. This gave hope that WSNs can also work inside metal train compartments.

For radio applications within reflective environments, a thorough understanding of radio wave propagation characteristics is essential for a functioning network. To obtain this knowledge, measurements need to be taken under different conditions. Research has shown that two parameters are particularly interesting: transmission output power and sensor node position. Hence the following research question:

> *"What are the radio wave propagation characteristics inside metal train compartments with different transmission output power and positions?"*

It is presumed that a lower transmission output power will cause less interference inside metal train compartments, as radio energy is dissipated quicker, thus reducing the probability that reflections occur. In the ideal case, the transmission output power is

adjusted to such a level that the receiving node is just within the radio range of the transmitter. This also reduces power consumption. The hypothesis of this thesis is formulated as follows:

> *"A sensor node transmitting at a lower output power causes less interference than one transmitting at a higher output power inside metal train compartments."*

Numerous measurements have been taken in different environments to help answer the research question and to prove/disprove this hypothesis. All measurements were taken in static environments to ensure that data are less polluted by human activities. Future research could include dynamic influences caused by human activities.

The remainder of the thesis is structured as follows: Chapter 2 discusses some of the related work to help place the thesis in the greater context. Chapter 3 gives a brief description of the tools used for the measurements. Measurements taken in De Biesbosch and the train metal compartments are discussed in Chapter 4 and 5. The final conclusion is presented in Chapter 6.

2 Related Work

This chapter discusses some of the relevant work related to this thesis. It forms the base knowledge for the chapters to come.

2.1 Wireless Sensor Networks Applications

A WSN consists of several sensor nodes, which form a network together. Sensor nodes are often called motes. They are mostly powered by batteries and have one or several sensors. A mote equipped with an actuator can interact with the environment.

WSNs are used for many different applications. They are often divided into different categories of applications. Each application has its own sets of requirements. (Kuorilehto et al., 2007, p. 15) puts WSN applications in three main categories: environmental monitoring, object tracking, and building monitoring. Object tracking is by far the most demanding in this set, because its data need to be updated frequently over the radio channel for accurate tracking. Radio is one of the most power hungry components of a mote. The reported operational lifespan of the listed applications in this category is one day. Applications in the environmental monitoring category and building monitoring category are less demanding and can reportedly last up to a few months. This is because environmental changes occur infrequently, thus reducing radio transmission. A different set of categories is presented in a survey of WSN applications (Arampatzis, Lygeros, & Manesis, 2005). Applications here are divided into five categories: military applications, environmental monitoring, commercial applications, human centric applications, and applications to robotics.

It is evident that applications which require frequent updates have a very short operational lifespan. This is because the radio transceiver on a sensor node consumes a lot more energy compared to other components on a sensor node. Reducing the usage of the radio transceiver will prolong the operational lifespan dramatically.

An example of an interesting WSN project is described by (Kevan, 2006) in a short online article. This project, *Loch Rannoch*, uses a WSN inside the engine room of an oil tanker to monitor vibrations of machinery. The data is used by a predictive maintenance system to prevent damages of the machinery. The environment of this project is similar to that of train compartments. The Loch Rannoch project will be referred to throughout this chapter.

2.2 Architecture

The OSI model (Figure 2-1) is the most widely used model to dissect the architecture of networks. It has its origin in Computer Networks. The model divides network communication into seven specialized layers. Each layer requests service from its lower layer and it also provides service to its upper layer (Tanenbaum, 2002). Most protocol implementations for WSNs are component-based and not layer-based. This is because a WSN is less complex and component-based implementation leads to less overhead in terms of code. Despite this component-based approach, developers of WSNs still use the model to describe protocol functionalities. Due to the simple nature of WSN applications, only the lower three layers are of interest. This section limits discussion to elements of the following layers: network layer, data link layer, and physical layer. The subject of energy consumption is predominantly present in the discussions of these layers.

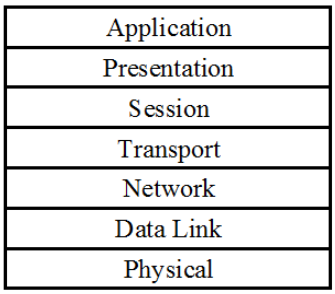

Figure 2-1. OSI Reference Model.

2.2.1 Network Layer

This section discusses primarily a technique often used by the network layer: multi-hopping. The network layer is responsible for routing data from sender to destination node. If a destination node is out of the reach of a sending node, the sending node can try to send its data via neighboring nodes. The neighboring nodes then try to relay the data to the destination node. This technique is called multi-hopping. Figure 2-2 illustrates how the coverage area is increased by means of this technique. The figure shows the sink[1] being outside the sender's radio range. Even if the sender's radio range is increased, their sight is still obstructed, making communication difficult if not impossible. The only way is to have the data relayed via neighboring nodes.

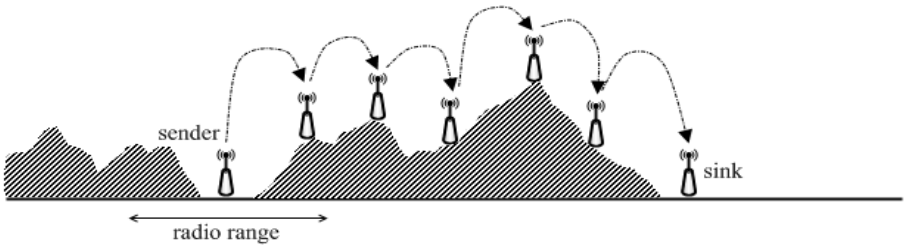

Figure 2-2. Increased coverage by means of multi-hopping.

[1] A data collecting node is often called a sink.

Besides being able to increase the coverage area, multi-hopping introduces another benefit. Radio transceivers can use multi-hopping to minimize power consumption, as communication between nodes at close distance requires less energy than nodes at greater distance. A simplified equation for energy consumption for transceivers with an omnidirectional antenna (see Section 2.3.2 Antennas) can be written as follows:

$$E = cr^2$$

E is the energy needed by a transceiver to transmit over a distance of r, c is a constant. This equation shows that energy consumption is proportional to r^2. For example, energy consumption increases by a factor of 16 when the distance is increased by a factor of four. Theoretically, it saves energy to use short multi-hops wherever possible. However, this does not necessarily hold true. When multi-hop is overused, wireless sensor networks can consume even more energy than on longer hops. This is because transceivers consume a good deal of energy at startup, thus possibly overshadowing the benefit of short hops.

The Loch Rannoch project uses multi-hopping in a mesh-network configuration to minimize interference. Instead of attempting to send a data packet directly to the sink, the data packet is relayed through its closest neighboring node. This procedure is repeated by every node on the path until the data packet finally arrives at the sink. How it is done that only the closest node receives the packet and not the nodes further away, is not elaborated by the author. It is likely that the transmission output power of the transceiver is adjusted to such a low level that only the closest neighboring node is able to listen to the transmissions. This makes sense, as this reduces disturbances caused by multipath effects (Section 2.2.3 Physical Layer) inside a confined environment. Much research has been done on reducing interference and energy consumption by adjusting transmission output power. (Lee, Kim, & Kim, 2006) illustrates how this principle works and how it can lead to an energy-minimal routing path. (Liu, Li, Zhou, & Li, 2007) describes an energy-aware protocol. This protocol reduces energy consumption of networks by adjusting the transmission output power while maintaining connectivity among motes. Several algorithms to construct an interference-aware topology are presented in (Li, Moaveni-Nejad, Song, & Wang, 2005). The aim of these algorithms is to minimize the average link interference of the topology. The measurements of this thesis will explore the effects of transmission output power on interference.

2.2.2 Data Link Layer

The data link layer is responsible for medium access control (MAC). It controls who gets access to the channel. A well-known problem is the *hidden and exposed terminal problem*. This occurs when terminals are unaware of the state of their neighboring terminals and it can cause packets to collide with each other or it can result in time slots not being used efficiently. This problem is well documented in (Tanenbaum, 2002, p. 295) and (Karl & Willig, 2005, p. 111). Many MAC protocols include algorithms to handle the issue of hidden and exposed terminal for WSNs.

One example of a MAC protocol is SMAC (Ye, Heidemann, & Estrin, 2004). The authors have identified four major sources of energy waste: collision, overhearing, control packet overhead, and idle listening. SMAC addresses all four wastes. One technique used is coordinated sleeping. This means that SMAC induces nodes into

periodic sleep to reduce idle listening. In SMAC, immediate neighboring nodes of the sender and receiver are put into sleep to avoid overhearing. This protocol introduces some latency but it is often acceptable for less real-time critical applications. A node in sleep mode consumes less energy than one in listen mode. On some nodes, the energy consumption between sleep mode and listen mode differs by a factor of 1000.

Another example of a MAC protocol for WSNs is LMAC (Van Hoesel & Havinga, 2004). This protocol is based on TDMA (Time Division Multiple Access). LMAC designates time slots to every node in the network, thus ensuring that only one node within a specific set nodes is allowed to transmit at any one time. This protocol saves energy by reducing the number of state switches, since there is no need for a handshaking mechanism.

2.2.3 Physical Layer

The thesis focuses mainly on this layer. The physical layer is concerned with the electrical aspects. WSNs are receptive to environmental changes. Link quality between nodes often deteriorates when their line-of-sight is obstructed. (Rappaport, 2002) defines three basic mechanisms that can impact radio wave propagation: reflection, diffraction, and scattering. Reflection is caused when radio waves hit a surface, which causes part or all of the radio energy to reflect into another direction. A perfect conductor reflects back all incoming radio energy without loss of power. Figure 2-3.a illustrates the principle of reflection. Part of the radio wave is reflected by surrounding metal. The receiving node then receives different copies of the same transmission from different paths. This is called the multipath effect. If there is line-of-sight between sender and receiver and radio waves are not reflected, then only one copy of the transmission is received, as illustrated by Figure 2-3.b. Multipath can result into two types of interferences as shown by Figure 2-4. Constructive interference enhances a radio wave, while destructive interference cancels out a radio wave.

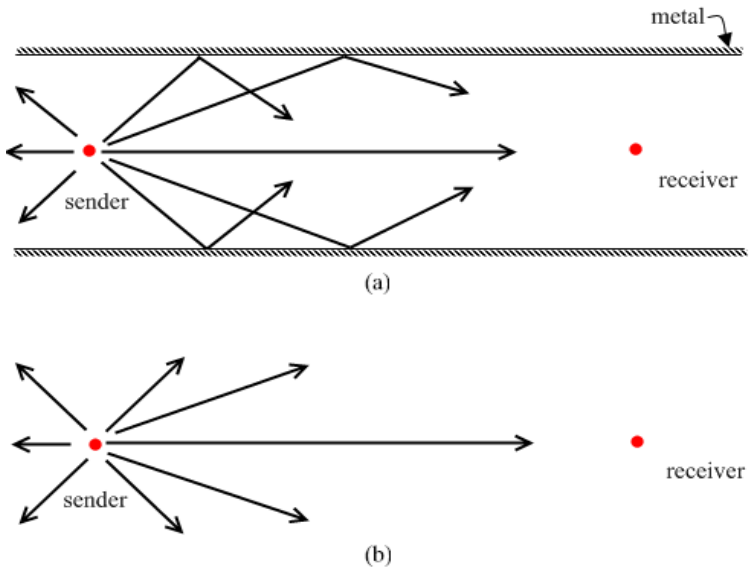

Figure 2-3. (a) Radio waves are reflected, causing multipath effect. (b) Radio waves propagate without being reflected.

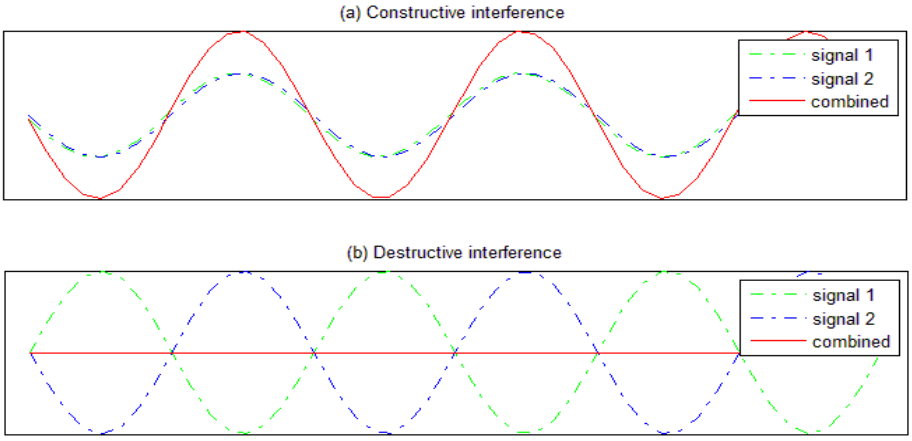

Figure 2-4. (a) Constructive interference; (b) Destructive interference.

(Puccinelli & Haenggi, 2006) and (Wu, Lee, Tseng, Jan, & Chuang, 2008) show that multipath fading is a spatial phenomenon and not directly a temporal phenomenon. Simply by repositioning nodes by a few centimeters causes changes in radio wave propagation characteristics. (Zhao & Govindan, 2003) and (Reijers, Halkes, & Langendoen, 2004) show that in an open space environment, such as a hockey pitch, radio waves reach the furthest without causing multipath effects. In confined environments, signal propagation is good up to a certain range and then becomes volatile. The region where signals become volatile is called the *grey area* and it is attributed to multipath effects. (Thelen, Goense, & Langendoen, 2005) observed that precipitation positively affects signal propagation in potato fields, while common sense would suggest that precipitation is bad for signal propagation. The authors attribute this positive effect to changes in the reflection coefficient of the potato canopy. Radio waves were better reflected under the potato canopy and that is likely to have caused constructive interference. This shows that multipath effect can be beneficial.

Interference might also originate from external noise sources. (Chandra & Bhawan, 2002) measured radio noise at 900 MHz and 1800 MHz from various sources inside a building. It is found that noise generated by fluorescent light fixture, elevator, and office equipments is likely to cause interference in those frequencies. Many sensor nodes operate at 868 MHz and 916 MHz.

2.3 Sensor Nodes

Sensor nodes form the backbone of every wireless sensor network. Dozens of different motes are commercially available at the moment. Sensor nodes are typically constructed from prefabricated components: transceiver, antenna, microcontroller, and memory. Depending on the bus structure, multiple sensors can be attached to a single node.

2.3.1 Transceivers

Transceivers give motes the ability to transmit and receive packets via ether. Popular transceivers for wireless sensor networks are the CC1000 (CC1000 single chip very low power RF transceiver, 2007) and the CC2420 (CC2420 2.4 GHz IEEE 802.15.4/ZigBee-ready RF transceiver, 2007). Most transceivers have an additional function to monitor Received Signal Strength Indicator (RSSI) values. This is used to retrieve noise floor values of a channel and also to retrieve the signal strength of incoming packets. Typically, RSSI values of incoming packets decrease as the distance to the transmitter becomes greater. The RSSI values need to be greater than the noise floor for any packets to be received.

Most transceivers operate on ISM (Industrial, Scientific, and Medical) frequencies, such as 315 MHz, 433 MHz, 868 MHz, 915 MHz, and 2.4 GHz. Low frequency radio waves are known to get around around obstructions better than high frequency radio waves due to their long wavelength.

When engaged in listening or transmission mode, transceivers usually consume more energy compared to any other components on the mote. (Van der Doorn, Kavelaars, & Langendoen, 2009) describes a prototype wakeup radio to overcome the problem of idle listening. This prototype uses a cheap ultra low-power radio on top of a regular transceiver. The transceiver remains in sleep mode and only wakes up if the wakeup radio receives a valid signal or when it wants to send a packet itself. This reduces the need for transceivers to listen to the channel at moments when no packets are being sent.

2.3.2 Antennas

Antennas have huge influences on how signals are received and transmitted. Popular antennas used today are ¼ wavelength monopole antennas and dipole antennas. Monopole antennas are used for the measurements in this thesis. Such an antenna has the property that its radio pattern shows no bias towards any horizontal direction. Figure 2-5 shows a schematic monopole antenna (a) with its radio pattern (b). Other antennas are available but are less common. For example, the Four-Beam Patch Antenna (FBPA) in (Giorgetti, Cidronali, Gupta, & Manes, 2007). It is claimed that FBPA increases the range in outdoor environments by more than 100 meters and it reduces interference in indoor environments, compared to regular omnidirectional antenna.

Different types of antennas show different characteristics. A methodology to assess

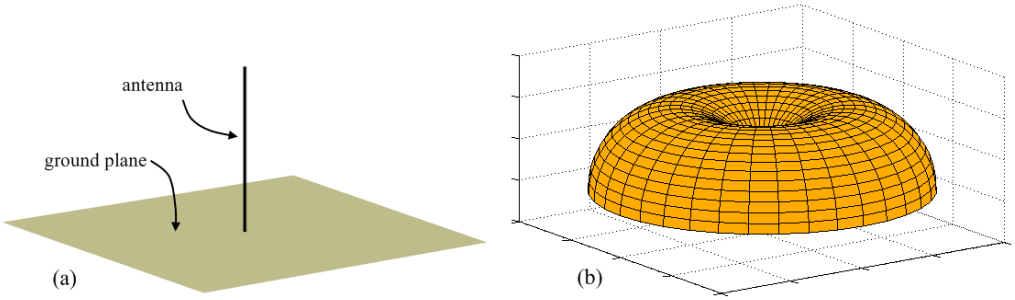

Figure 2-5. (a) Schematic drawing of a monopole antenna attached to a ground plane. (b) Theoretical radiation pattern of a monopole antenna.

antenna performances is presented in (Buckley, Aherne, O'Flynn, Barton, Murphy, & O'Mathuna, 2006). This method requires no anechoic chamber or special equipments. Two motes are used: one functions as sender and the other as a receiver. Tests are conducted on a remote football field to minimize the effects posed by objects. The sending mote sends out 100 packets while the receiving mote records the number of packets it receives. This procedure is repeated multiple times, each time with a different horizontal separation distance between the sender and the receiver. The results provide some intuitions on antenna behavior and help to identify cases in which more specific equipments are required. A similar, but more comprehensive approach is described by (Halkes, 2004). One transmitter and a row of receivers are used. The directionality of the mote is approximated by rotating the transmitter in various orientations while the receivers keep track of the packet reception rate. Antenna radiation patterns can be approximated using this method. An adapted version of this methodology is used in this project.

2.3.3 Dimensions

The dimensions of motes are small - generally just a few square centimeters. Figure 2-6.a and Figure 2-6.b depict the popular Crossbow MICA2 and the SOWNet T-Node, respectively. In the figures, the nodes are both equipped with a ¼ wavelength antenna. The standard hardware components are also very similar. Both nodes are equipped with an Atmel ATMega128 microcontroller and a Chipcon CC1000 transceiver. While motes are usually small, this advantage is often overshadowed by the size of the batteries required to power them. Though transistor size has been drastically reduced over the years, battery power density has not improved significantly. Batteries nearly always outweigh and outsize motes. The measurements in this thesis are taken with T-Nodes.

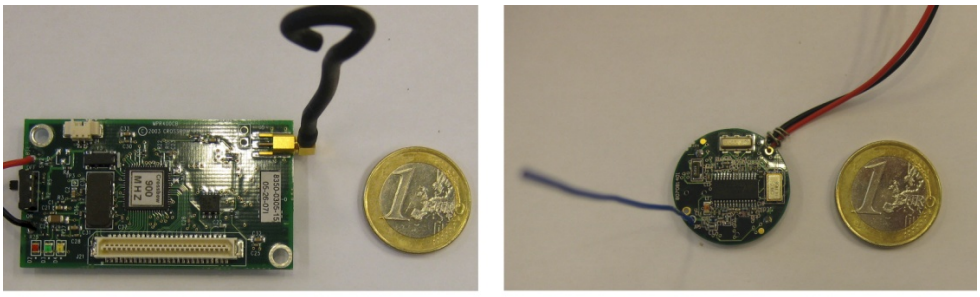

(a) (b)

Figure 2-6. (a) Crossbow MICA2 ; (b) SOWNet T-Node

2.4 Received Signal Strength Indicator

Received Signal Strength Indicator (RSSI) can provide valuable information on the wireless channel. RSSI value is used to quantify the signal strength of incoming packets and of the noise floor. The RSSI value of incoming packets usually decreases as the distance between the transmitter and receiver becomes greater. Obstructions may

attenuate radio waves. (Rappaport, 2002, p. 158) shows a list of common building materials and their average signal loss measurements. An all-metal obstruction results in a loss of 26 dB, while a concrete wall results in a loss of 13 dB. The RSSI value of an incoming packet should at least surpass the noise floor value, for it to get accepted. If the RSSI value of an incoming packet is near or below the noise floor value, then it becomes difficult to impossible to distinguish the data transmission from noise.

RSSI obtained from the transceivers are not accurate. Datasheets for the CC1000 transceiver (CC1000 single chip very low power RF transceiver, 2007) and the CC2420 transceiver (CC2420 2.4 GHz IEEE 802.15.4/ZigBee-ready RF transceiver, 2007) both report an accuracy error of ±6 dB. (Alippi & Vanini, 2004) shows that this accuracy is more likely to be ±7 dB for the CC1000 transceiver on a MICA2 mote. The main source of error is attributed to different realizations of the MICA2 motes.

RSSI values are used for various applications. (Lim & Wong, 2006) uses the MICA2 nodes to show the relation between RSSI value, distance, packet reception rate, and transmission power. The authors have observed the existence of a negative correlation between distance and RSSI. Further, a positive correlation exists between transmission power and RSSI. (Srinivasan & Levis, 2006) claims that RSSI is also a good estimator for link quality. Here, a CC2420 is used to show the existence of a threshold at -87 dBm. For RSSI values above this threshold, packet reception rates are at least 85%. Packet reception rates vary between 0% to 100% for RSSI values below this threshold.

2.5 Modeling Wireless Sensor Networks

The iteration of implementation and field testing is a very time consuming practice. This is why researchers have resorted to the use of mathematical models and network simulators for WSNs. Implementation of WSNs can be modeled and tested rigorously using computers. If tests yield satisfactory results, the whole setup can then be tested on the field or deployed directly in the environment. This method only works if statistical data for the environment are available. If the environment is new, then new statistical data of radio wave propagation must be collected for this method to work properly.

2.5.1 Mathematical Models

Models are often used to simulate radio fading. A model is a simplification of the reality and it allows researchers to test protocols, without the need of troublesome field tests. (Hekmat, 2006) describes the decomposition of signal fading into three components: large scale, medium scale, and small scale. The large scale component is concerned with the dependence of the mean signal strength on the separation distance between a transmitter and a receiver. The distance is typically a few meters to thousands of meters. The medium scale is concerned with the variation of signal strength, given the distance between a transmitter and a receiver. Finally, the small scale component relates to the rapid variation in signal strength over distances within a few wavelengths or over time periods within a few seconds.

This thesis excludes the medium and the small scale component. For the medium scale component, a large quantity of data is needed. This seems unrealistic given the

limited time and availability of the train compartments in which measurements are taken. The small scale component is excluded, because it is known that the small scale fading effects are quickly averaged-out over time.

Various models are available for large scale fading (Rappaport, 2002). However, only the *log-distance path loss model* is considered in this thesis. The reason for this is that the metal train environment is relative unknown and this model is less environment-specific. This model can be expressed as a function of distance

$$PL(d) = PL(d_0) + 10nlog(\frac{d}{d_0})$$

where $PL(d)$ is the path loss at distance d, d_0 is the reference distace, $PL(d_0)$ is the path loss at d_0, and n is the path loss exponent. d_0 is usually chosen to be 1 meter. $PL(d_0)$ can either be measured or estimated. Different environments have different values for n. The path loss exponent is 2 for free space and 4 to 6 for inside buildings with no line-of-sight. The estimated receive power at a given distance is expressed as

$$P_r(d) = P_t - PL(d)$$

where $P_r(d)$ is the estimated received power at distance d and P_t is transmission output power. Figure 2-7 illustrates an example of four estimated receive powers, $P_r(d)$, obtained by the log-distance path loss model under various exponent values. The log-distance path loss model is used to fit some of the measurement data taken during the course of the project. The data will facilitate future researchers to simulate radio wave propagation in a train compartment environment.

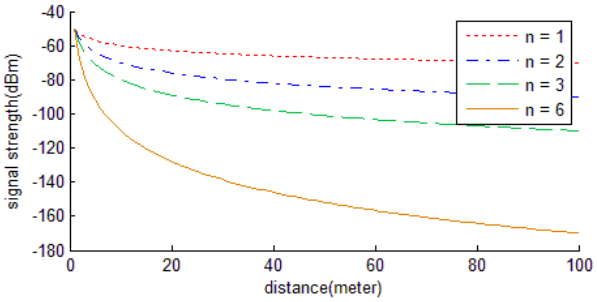

Figure 2-7. Example of estimated received power at distance d under various path loss exponents. $PL(d_0) = -50$, $d_0 = 1$.

2.5.2 Simulators

Simulators are used to simulate WSNs behavior in different environments under various conditions. They allow developers of protocols to test their implementation in virtual WSNs, without having to use any physical nodes. Source codes for nodes often need to be converted to another language, which the simulator understands.

Most simulators for WSNs allow users to test implementations in the network layer, data link layer, and the physical layer. Networks consisting of tens to hundreds of nodes can be simulated at once. TOSSIM (TinyOS, 2008) and MiXim (Köpke, et al., 2008) are just some of the widely available simulators.

2.6 Discussion

This chapter has not only shown the benefits of WSNs but it has exposed some of their limitations. Both energy supply and environment are limiting factors to WSNs. Operational lifespan of motes is directly dependent on energy consumption. Reflective environment can cause multipath effects and obstructions may even make communication impossible. Multi-hopping seems to be a promising technique to overcome some of these issues.

The choice of hardware is important. Different hardware may show different characteristics. This is especially true for antennas. Furthermore, the choice of battery influences the possible locations for node placement. Smaller batteries yield more possibilities where nodes can be placed. However, a smaller battery usually means a shorter operational lifespan. Transceivers consume a lot of energy. A mote lasts longer when its transceiver is less active.

Creating a WSN from scratch requires much effort. Propagation models and simulators can ease some of the pain. Models let developers to estimate the behavior of WSNs. Simulators allow implementation of WSNs to be tested in various virtual environments under different conditions. However, statistical data are always needed to fine tune the models and simulators. These data are collected in an open field and in train compartments. Their results are discussed in Chapter 4 and Chapter 5.

3 Measurement Tools

This chapter discusses the hardware and software used during the measurements. Data are retrieved using sensor nodes in combination with customized software.

3.1 SOWNet T-Node

The measurements are performed on motes produced by SOWNet. These sensor nodes, called T-Node (SOWNet Technologies, 2008), are equipped with a Chipcon CC1000 transceiver together with an Atmel ATMega128 controller. Figure 3-1 depicts the T-Node in the lower right corner and the USB interface on top. These motes are the size of an euro coin. The T-Nodes run on an operating system called TinyOS (TinyOS, 2008). It is designed specifically for sensor nodes and it is component based.

The Chipcon CC1000 has a RSSI accuracy of ±6 dB according to its datasheet (CC1000 single chip very low power RF transceiver, 2007). The operational radio frequency is set to 868 MHz. A regular solid core steel cable with a diameter of 0.2 mm is used as a monopole antenna. This antenna has a length of 8.6 cm, which corresponds to a ¼ wavelength. The choice for this type of antenna was made, based on the fact that this antenna is easily and cheaply produced. Furthermore, monopole antennas are known to show no bias in horizontal directions, as shown in Figure 2-5.b.

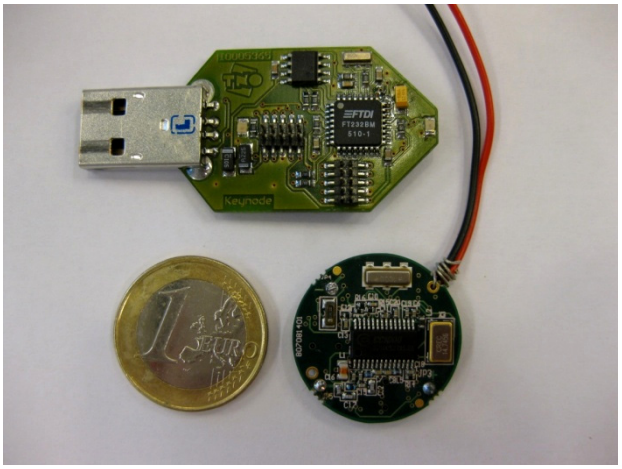

Figure 3-1. SOWNet USB interface and T-Node

The USB interface is used to upload codes to nodes. A node attached to the USB interface can be controlled by a laptop. During the measurements, always one node is attached to this USB interface to serve as a transmitter. This transmitting node is also used to issue commands to receiving nodes. Furthermore, data stored on the receivers are transferred via this node to the laptop.

The transmitter has its energy supplied by the laptop, while the receivers have their energy supplied by batteries. Initially, cheap lithium batteries were used to supply the receivers with energy. However, it was discovered that these lithium batteries were not able to cope with the peak current demand of the T-Nodes. On advice of SOWNet, regular AA alkaline batteries were used to replace the lithium batteries. The alkaline batteries were fully capable of coping with the peak current demand.

3.2 TNode Console

Much effort has been invested in creating a suitable software platform for the measurement campaign. TNode Console has been created for this means. It consists of NesC[1] codes for the T-Nodes and Java codes for the computer interface (Figure 3-2). The codes for the transmitter are different from the codes for the receivers.

The greatest asset of TNode Console is the ability to initiate different types of test wirelessly, without the need to re-flash the mote for each type of test. Data from receivers are also retrieved wirelessly. These abilities are crucial, as it allows users to take multiple tests without moving the motes, hence eliminating undesired effects

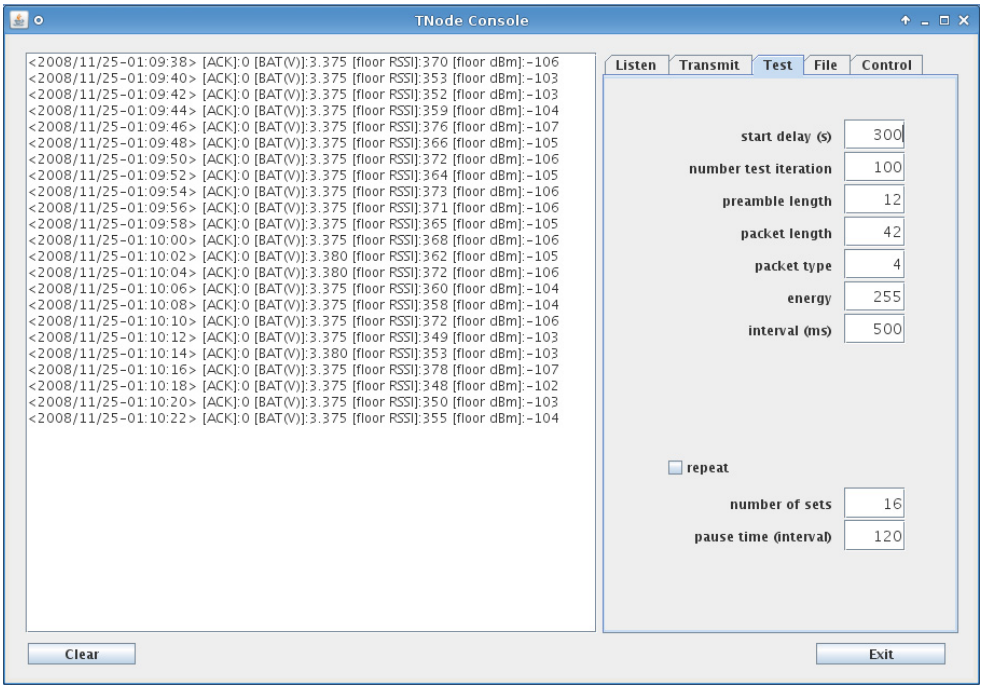

Figure 3-2. Screenshot TNode Console's GUI

[1] NesC is the language used by TinyOS. It is a variant of the language C.

caused by mote displacements.

TNode Console is able to perform two different kinds of test. The first test listens to the radio channel for noise at user-defined time intervals. This test determines the noise floor of the channel.

The second test involves packets. The transmitter, which is attached to the USB interface, sends out a set of packets at a predefined time. The receivers listen to the channel and log everything which has a preamble byte[1] followed by a sync byte[2]. The user can define the following variables for the transmitter: preamble length, packet content, transmission output power, number of packets, and time interval for subsequent transmissions. The user has a choice of four different packet contents. The first type of packet contains a sequence of zero bits, while the second type contains a sequence of one bits. The third type of packet contains a sequence of alternating one and zero bits. Finally, the fourth type of packet contains a sequence of ones and zeros at random order. These four types of packets allow researchers to examine the influence on radio wave propagation for different bit sequences. The length of these packets is adjustable by the user.

The standard codes of TinyOS have been painstakingly altered to gain control over the packet layout. TinyOS inserts a standard header and footer to every packet it sends. We have altered this function to give TNode Console full authority over the content of the packet. Furthermore, incoming packets which fail the CRC check are discarded by TinyOS by default. This function has also been removed for the TNode Console. It is able to accept packets as long as it has at least one preamble byte followed by a sync byte. This feature is necessary in order to examine the nature of corrupted packets.

Other features of TNode Console include remote clock synchronization between receivers and transmitter, and the ability to request at real-time the noise floor value and battery status from the receivers.

The features of TNode Console can be easily extended for new types of tests. The current version of TNode Console is sufficient for the measurements in this project.

[1] A preamble byte precedes the data packet and is used to synchronize communicating nodes. It usually contains a sequence of alternating one and zero bits.

[2] A sync byte has the form of 11001100 or 00110011.

4 De Biesbosch

De Biesbosch is a Dutch national nature reserve, located near Dordrecht. A secluded open field within this reserve is chosen for the benchmark measurements. This open field ensures line-of-sight between the transmitter and the receivers. The nearest urbanization is kilometers away and only a very few people visit this area per day.

The measurement data from this environment is used as comparison for the train compartments data in Chapter 5. The data in this open field are fairly predictable due of the lack of human activities and obstacles around the measurement area. Several days were required to take the measurements.

4.1 Measurement Setup

During the entire length of the measurement campaign in De Biesbosch, the same sensor nodes were positioned at the same distance from the transmitter. This is because of the assumption that radio wave propagation degrades gradually as distance increases. Any irregularity in the data curve can then directly be contributed to the T-Nodes. Table 4-1 lists the node IDs and their distance from the transmitter. Unlike (Halkes, 2004), nodes are placed closer together near the transmitter. The reason for this is that the area closer to the transmitter is more interesting for tests with low transmission output power. Low transmission power output gives nodes a shorter range. Our hypothesis states that low transmission output causes less interference.

Table 4-1. Separation distance between transmitter and receivers

node ID	distance to transmitter (meter)	node ID	distance to transmitter (meter)	node ID	distance to transmitter (meter)
1	1	11	12	21	35
2	2	12	14	22	40
3	3	13	16	23	45
4	4	14	18	24	50
5	5	15	20	25	55
6	6	16	22	26	60
7	7	17	24	27	70
8	8	18	26	28	80
9	9	19	28	29	90
10	10	20	30	30	100

30 T-Nodes were used as receivers and one T-Node functions as a transmitter. The transmitter is connected to a laptop via a USB interface. The receivers take their energy from batteries while the transmitter takes it from the laptop via the USB interface. All nodes, including the transmitter, are placed on PVC poles at a height of about 0.7 meter above ground. The nodes are aligned along an imaginary line of 100 meters. The transmitter is placed at one end of this imaginary line. Figure 4-1 depicts the measurement setup as described.

Figure 4-1. The right most pole holds the transmitter, which is connected via a USB cable to a laptop. 30 receivers are positioned along a line of 100 meters.

The receivers are all oriented in the same direction with their antenna at upright position. Only the transmitter is allowed to change orientation during the measurements as explained in the next sections.

The remainder of this chapter describes the individual measurements. Each type of measurement requires a different methodology, while the distances between the receivers and transmitter always remain the same.

4.2 Horizontal Directionality

This test is designed to gain knowledge on the directionality of the T-Nodes at a horizontal position. The result will expose any bias if it exists at all. The outcome provides aid in determining how nodes are best placed inside the train compartments of Chapter 5.

4.2.1 Methodology

This methodology is similar to that of (Halkes, 2004). The difference lies primarily in the density of the receivers. In this setup, relatively more receivers are present near the transmitter. The reason for this was explained in Section 4.1.

The transmitter is leveled horizontally and rotated in 16 different horizontal angles (Figure 4-2.a). At each angle, the transmitter broadcasts 100 packets at intervals of 500

ms between transmissions. Each packet carries 42 bytes of content, containing a predefined random sequence of ones and zeros. The packet is preceded by 12 bytes of preamble. Standard TinyOS codes put six preamble bytes. However, this test uses 12 bytes to observe the influence of preamble bytes on packet reception rate (PRR). The entire packet is transmitted at maximum transmission output power (5 dBm). The measurements are repeated three times resulting in 300 packets per angle. The receivers listen constantly to any incoming transmissions. Each receiver keeps a log of the number of the received preamble bytes, the RSSI value, and the received content. Note that only complete preamble bytes are logged. A byte with only part of a preamble does not count as a preamble byte.

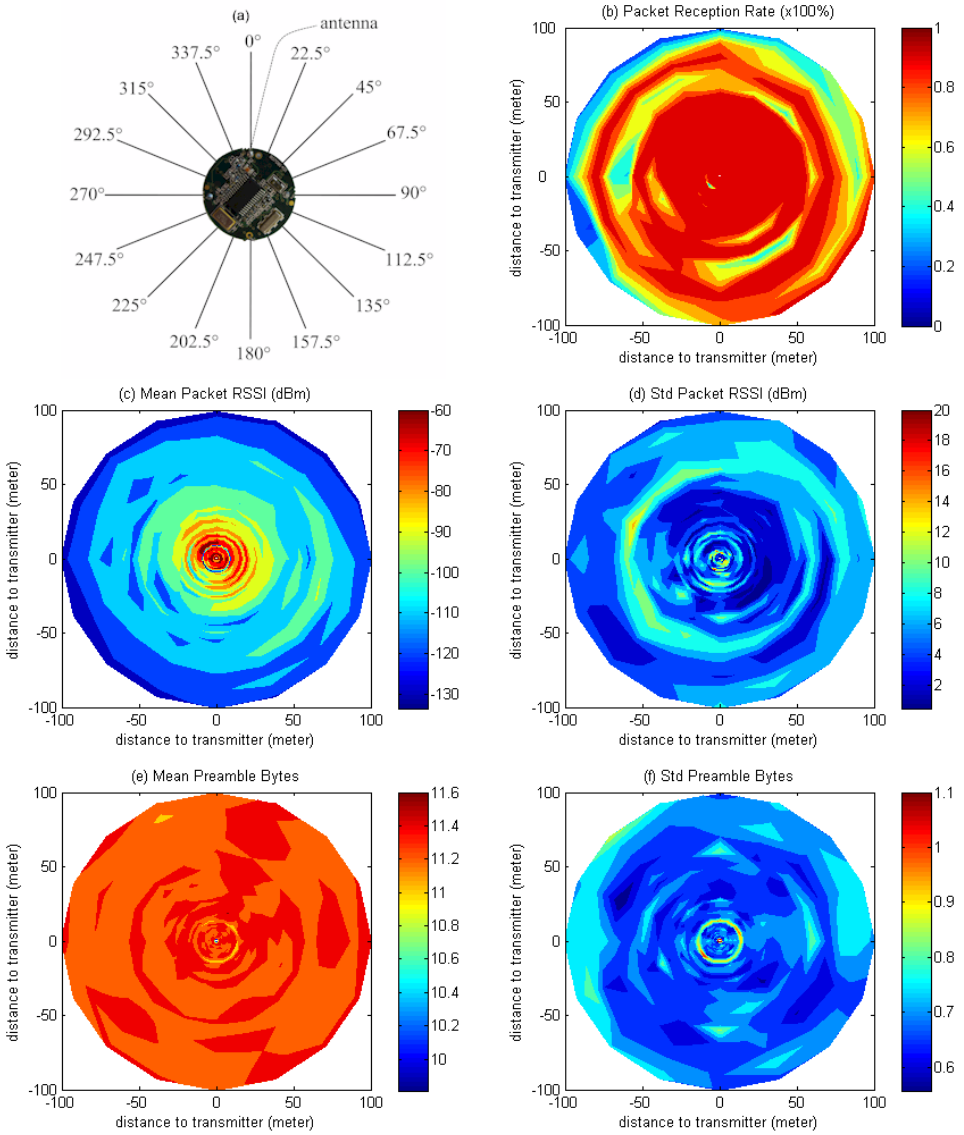

Figure 4-2. The transmitter is oriented in 16 different angles; (b) packet reception rate; (c) mean packet RSSI value; (d) standard deviation of packet RSSI value; (e) mean number of received preamble bytes; (f) standard deviation of received preamble bytes.

4.2.2 Data Analysis

Figure 4-2 depicts the measurement results in five different plots. The angle of each individual plot corresponds to the angle of orientation of the transmitter (Figure 4-2.a). Early on during the tests, it was found that the node at 9 meter malfunctions. This node had difficulties communicating with the transmitter, even at close proximity. This led to irregularities visible in the plots at 9 meter.

The plots in Figure 4-2 show no obvious bias towards any particular direction. This assertion can be extracted from the circular patterns, which are easily identified from the plots for PRR (Figure 4-2.b) and mean packet RSSI (Figure 4-2.c). This was expected as it is known that monopole antennas do not favor any particular direction. It is difficult to relate distance to PRR by means of Figure 4-2.b. A sharp drop of PRR is observed in the far end of the left hemisphere. However, this drop is less evident in the right hemisphere. The radio waves propagate quite well up to 100 meters; no measurements were taken beyond 100 meters. Figure 4-2.c shows a strong relation between the reduction of RSSI and the increase of transmitter-receiver distance. However, variations of these values fluctuate strongly (Figure 4-2.d).

Figure 4-2.e shows that the number of preamble bytes received by the receiver is on average around 11.3. Recall that the transmitter precedes every packet with 12 bytes of preamble. Figure 4-2.f shows that the standard deviation is around 0.76. These two plots suggest that as little as two preamble bytes might be enough to synchronize the receivers with the transmitter. A minimum of two bytes are needed, because part of the first preamble byte might be discarded as noise due sampling. Figure 4-3 illustrates an example of this. The node samples the channel in chunks of eight bits. Part of the first preamble is present in the second sample. However, this sample is discarded, as it does not conform to the sequence of a preamble. The sequence of the preamble is only detected in the third sample. Reducing the number of preambles bytes will prolong the operational lifespan for nodes, especially for cases when only small packets are sent.

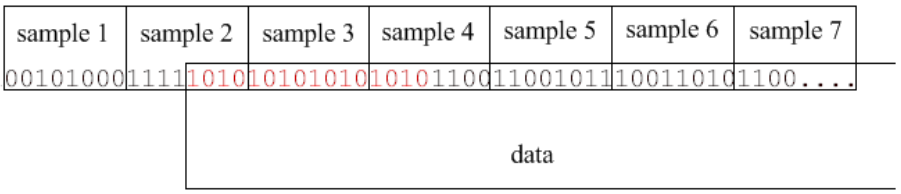

Figure 4-3. The channel is being sampled in chunks of eight bits. The data is preceded by two bytes of preamble, shown in red here.

Besides the unusual circular line at 9 meter, another one is also visible at 60 meter distance in the plots. In the beginning, it was unclear as what caused this line to appear. It was assumed that this line was caused by a hardware issue. This assumption is confirmed in the next section.

4.3 Antenna Angle

This section seeks to provide insights on the effect of the ground plane on radio wave propagation and the characteristics of radio wave propagation under various antenna angles. The outcome of the tests will help determine how nodes are best placed in the train compartments of Chapter 5.

4.3.1 Methodology

The methodology is similar to that of the previous experiment. However, the transmitter is not rotated horizontally. Instead, its antenna is tilted vertically in various angles. There are two sets of tests. In the first set, the entire node is tilted in nine different angles towards and away from the receivers (Figure 4-4.a). Note that the antenna is perpendicular to the ground plane of the T-Node in this set. In the second set, the ground plane is kept leveled. The antenna is bent in nine different angles towards and away from the receivers (Figure 4-4.b).

The two sets of tests are carried out after each other in a single session. The tests were later repeated in a second session. A total of 200 packets per angle per set were sent. The parameters for the transmissions are exactly the same as for the previous experiment.

4.3.2 Data Analysis

Figure 4-4 depicts some of the results of these measurements. Similar to the first experiment, circular lines are shown at 9 meter and 60 meter. The dark line at 60 meters indicates that a mayor breakdown of the transceiver has occurred. No packets were received at this distance. Separate tests have shown that this problem is caused by hardware fault. This node had difficulties communicating with other nodes, even at close proximity.

The plots in the left column of Figure 4-4 are obtained by tilting the ground plane towards and away from the receivers. The antenna is kept perpendicular to the ground plane of the T-Node. The plots in the right column are obtained by keeping the ground plane horizontal, while bending the antenna towards and away from the receivers.

The plots of both columns are very alike. From this, we conclude that the ground plane has no to little effect on radio wave propagation characteristics in this environment. The results of this experiment are similar to the first experiment. The PRR is still fairly good up to 100 meters. A strong relation between the reduction of RSSI and the increase of transmitter-receiver distance is evident. The plots for the preamble and its standard deviations are left out in the figure because they do not add any new facts. The average number of received preamble bytes is 11.3 with a standard deviation of 0.76. These values are exactly the same as reported in Section 4.2.2.

The two columns of Figure 4-4 also indicate that antenna orientation has no influence on reception. This contradicts the belief that signals are weaker in the length of the antenna, as is shown in Figure 2-5.b by the trough in the middle of the radiation pattern. If this was true, then Figure 4-4 would show dips in signal strength at -90° and 90°. This is clearly not the case. It is assumed that this observation is caused by ground reflections. The radio waves are likely to have reflected off the ground to the receivers.

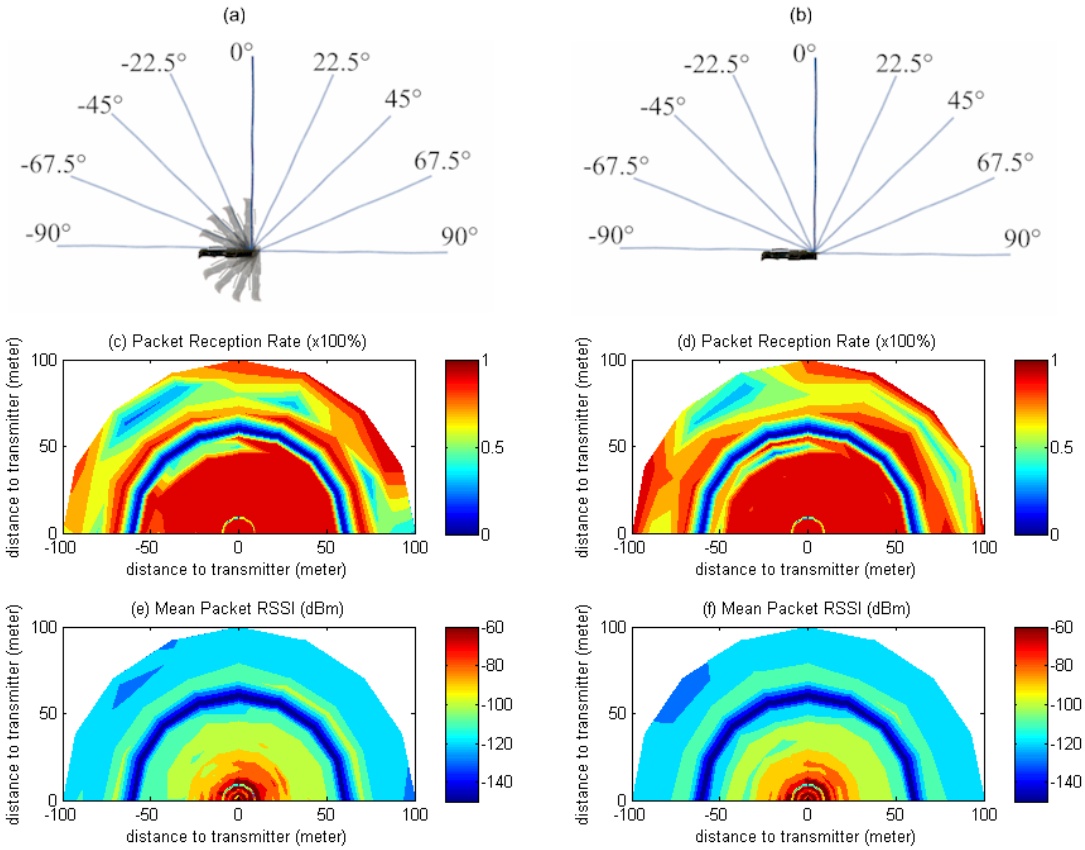

Figure 4-4. (a) Ground plane is tilted in nine different angles, while the antenna is kept perpendicular to the ground plane; (b) ground plane is kept horizontally, while the antenna is bent in nine different angles; (c) packet reception rate under various ground plane angles; (d) packet reception rate under various antenna angles; (e) mean packet RSSI value under various ground plane angles; (f) mean packet RSSI value under various antenna angles.

4.4 Power Transmission

This section examines the effect of various transmission output powers. The results are later compared with similar data of train compartments in Chapter 5. This section explores the relation between transmission output power, PRR, RSSI, and preamble length. The data for RSSI is later fitted onto the log-distance path loss model.

4.4.1 Methodology

The setup of the nodes is similar to the first experiment. The receivers are positioned in a line with the transmitter at one end of this line. The transmitter remains stationary for the entire duration of the test. Its antenna is at upright position.

The transmission variable is similar to the first experiment, except for its transmission output power. During each test session, the transmitter broadcasts 16 sets of 100 packets at 16 different transmission output power levels. Table 4-2 lists the available

output power range and its current consumption. Output values with an asterisk (*) are included in the tests.

Table 4-2. Transmission power range and current consumption on the CC1000 transceiver operating at 868 MHz. Source: (CC1000 single chip very low power RF transceiver, 2007)

output power (dBm)	**current consumption (mA)**	**output power (dBm)**	**current consumption (mA)**
-20*	8.6	-7*	10.8
-19*	8.8	-6	11.1
-18*	9.0	-5*	13.8
-17*	9.0	-4*	14.5
-16*	9.1	-3*	14.5
-15*	9.3	-2	15.1
-14*	9.3	-1*	15.8
-13*	9.5	0	16.8
-12*	9.7	1*	17.2
-11	9.9	2	18.5
-10*	10.1	3*	19.2
-9*	10.4	4	21.3
-8	10.6	5*	25.4

4.4.2 Data Analysis

A selection of the results is given in Figure 4-5. Recall that the receiver at 9 meter malfunctions. The black dots in the top of each plot show the location of the receivers. The first column shows the signal strength of incoming packets vs. the distance to the transmitter. The second column shows the number of received preamble bytes and PRR vs. the distance to the transmitter.

Each row of plots represents data at different output power. The output powers are 5, -1, -5, -10, -15, and -20 dBm, from the first row to the last. The dotted line in the first column is the path loss model curve. The RSSI value at 1 meter is used as reference for the model. The path loss exponents are obtained by calculating the minimum mean square error between the model and the data.

The graphs for packet RSSI show a gradual drop in received power as the distance between the receiver and transmitter increases. The path loss model fits fairly well on the measured signal strength data. The path loss exponent is close to the free space exponent (i.e. 2) for higher transmission output power. A summary of path loss exponents and transmission output power levels are listed in Table 4-3. These values are extracted from measurement data collected in this section.

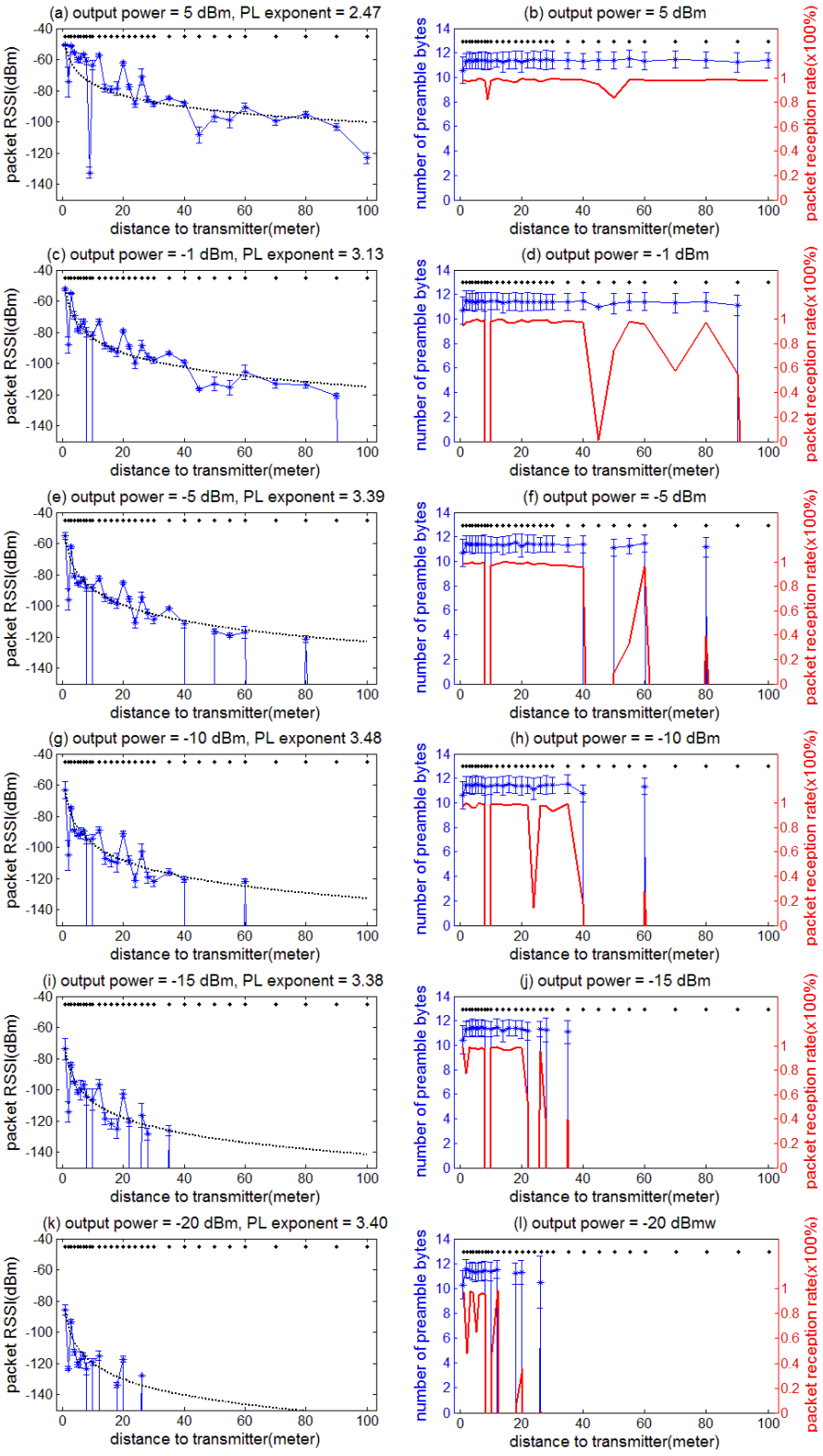

Figure 4-5. Left column: RSSI values vs. distance to transmitter. The path loss model is projected on top of the measurements. Right column: number of received preamble bytes (blue) and PPR (red) vs. distance to transmitter.

Table 4-3. Path loss exponents for various output power.

output power (dBm)	path loss exponent	output power (dBm)	path loss exponent
< -20	3.61	-9	3.50
-20 ~ -19	3.40	-7	3.47
-18 ~ -17	3.29	-5	3.39
-16	3.33	-4 ~ -3	3.31
-15 ~ -14	3.38	-1	3.13
-13	3.41	1	2.99
-12	3.43	3	2.84
-10	3.48	5	2.47

The second column of Figure 4-5 shows that the received preamble length is on average 11.4 bytes. This value also holds for low PRR. This strengthens the assertion that two preamble bytes are sufficient. The number of received preamble bytes drops immediately to zero when the packet RSSI drops below a certain threshold. At this point, PRR also drops to zero. This implies that whenever packet reception is possible, preambles are always received in full. The relation between packet RSSI and PRR is shown in Figure 4-6. This figure shows that PRR is at least 83.5% for RSSI values larger than the threshold of -97 dBm.

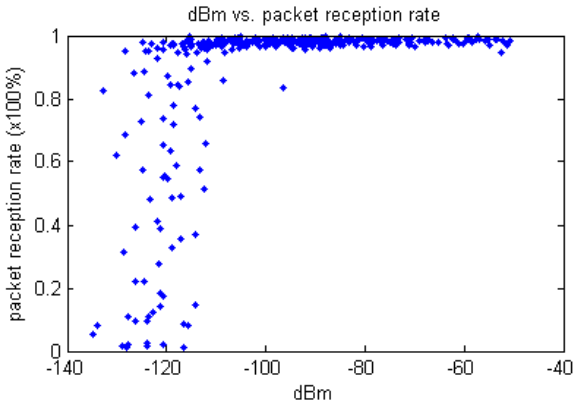

Figure 4-6. RSSI vs. packet reception rate.

4.5 Discussion

The tests in this section provide important insights on how the T-Node behaves in a free space environment such as De Biesbosch. The data in this section serves to facilitate the placement of nodes in Chapter 5.

The tests have shown that the horizontal orientation of nodes is not biased in any particular direction. Also, the vertical orientation of antenna has shown no sign of bias. This can be caused by reflection of radio waves off the ground. The tests with bent antennas and tilted transmitter yield similar results. This implies that an antenna can be bent without influencing the reception of radio waves. This knowledge is used in

Chapter 5 for placing the nodes in the train interior. Note that all tests were carried out with T-Nodes. It is fully possible that a different hardware might yield different outcomes.

It is found that RSSI can be approximated by the log-distance path loss model. However, the path loss exponent differs for different transmission output powers. Path loss for lower transmission output powers can be estimated with a larger path loss exponent. The path loss exponent for maximum transmission output power is 2.47. This value is close to the path loss exponent of 2 for free space environment.

In standard TinyOS, each radio transmission is preceded by six bytes of preamble. The tests in this environment suggest that increased preamble bytes do not yield better reception rate. The tests indicate that as little as two preamble bytes are enough. Using fewer preamble bytes saves energy and could potentially increase the operational lifespan of nodes. This is not further explored, as this is not included in the scope of this thesis.

The measurement data have shown that packet reception rate is related to signal strength. It is discovered that packet reception rate is at least 83.5% for signal strength exceeding -97 dBm. Packet reception rate varies from 0% to 100% for values below this threshold.

Finally, another important observation is that individual nodes may yield different results. This has also been reported in (Alippi & Vanini, 2004). The extreme cases were the nodes at 9 meter and 60 meter, which had difficulties receiving packets.

5 Train Compartments

This chapter presents the results of tests taken in metal train compartments. The train compartment is highly metallic and only a few cases of WSN deployment in metallic environments are known in literature. This makes the train an even more interesting environment for the study of WSNs. The measurements of this chapter provide insights on radio wave propagation characteristics in metal train compartments.

Two different sets of tests are described in this chapter. The first set of tests determines the effects caused by antenna orientation. The second set of tests determines the overall radio wave propagation characteristics across a single train compartment and between two train compartments. This chapter starts with the description of the general methodology for the experiments.

5.1 Measurement Setup

All measurements mentioned in this chapter are performed in the compartments of the V-IRM2 (Figure 5-1.a). This model is chosen for the tests, because it is widely used by the Dutch national rail carrier. If any WSN application is developed for passenger trains, then it is most likely to be deployed in this model first.

The tests are done on empty compartments without the presence of people in them. This helps to eliminate the effects caused by human activities, making it easier to clarify certain phenomena if present in the data. Future tests could include human elements for more realistic measurements. The train remains stationary for the entire duration of the experiments.

Unlike the setup for De Biesbosch, the nodes are placed at irregular distances away from the transmitter. They are only placed at locations where they can potentially be

(a) (b)

Figure 5-1. (a) V-IRM2; (b) node and battery attached to the interior with tape.

placed, if they were deployed in a real WSN application. This is why the nodes are not suspended in the air, as in the case of De Biesbosch. The antenna is bended so it can be placed flat against the interior of the compartment. Figure 5-1.b depicts the placement of a node together with its battery pack on a ceiling panel. In a real WSN application, this node can be placed behind the panel.

The nodes are attached to the interior with tape. Some receivers might have a line-of-sight with transmitter, however most receivers do not have line-of-sight with the transmitter. Only one transmitter is used during each test, while all other nodes function as receivers.

The packet content is exactly the same as for the tests in the previous chapter. The content of the packet is a predefined random sequence of one and zero bits. A packet is preceded by 12 bytes of preamble. The transmitter broadcasts packets at 16 different transmission output power levels. 100 packets per transmission output power level are broadcasted. A total of 1600 packets are transmitted per test session.

5.2 Antenna Directionality

This section examines the effects of antenna orientation on radio wave propagation. Section 4.3 Antenna Anglehas shown that antenna orientation is irrelevant for De Biesbosch. This section checks whether that observation holds true for metal train compartments as well.

5.2.1 Methodology

The receivers are placed at 15 different locations in the lower deck of the compartment, as shown in Figure 5-2. Three locations are on the ceiling and 12 are underneath the seats. The red dot in the figure represents the location of the transmitter. The transmitter is located underneath a seat. Each receiving location holds two nodes with different antenna orientations. One node has its antenna directed perpendicular to the length of the compartment (Figure 5-3 left). The other node has its antenna directed parallel to the length of the compartment (Figure 5-3 right). The two nodes are at close

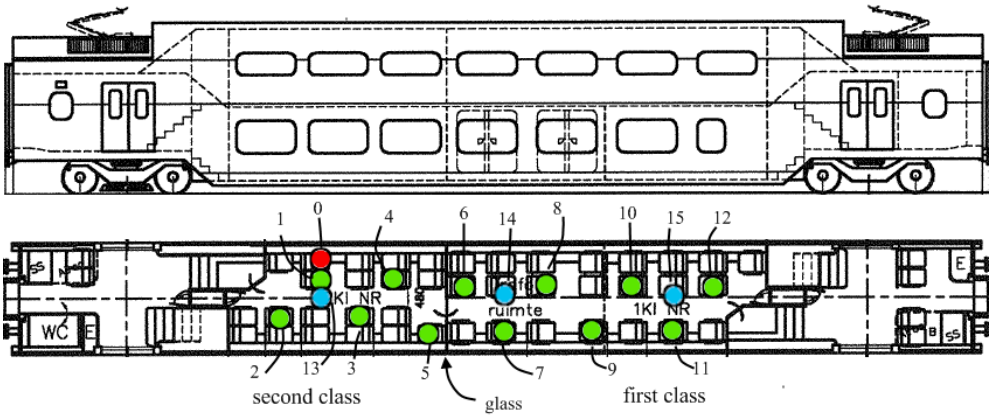

Figure 5-2. Lower deck. The locations of the nodes are numbered. Red: location of transmitter underneath the seat. Green: location of receiver underneath the seat; Blue: location of receiver on the ceiling.

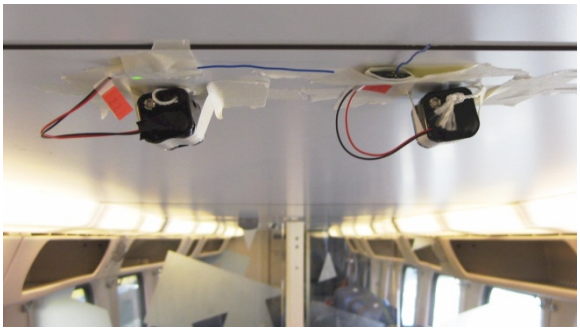

Figure 5-3. Receivers attached to ceiling. Left: antenna perpendicular to the length of the compartment. Right: antenna parallel to the length of the compartment.

proximity of each other. None of the receivers has line-of-sight with the transmitter in this experiment. The distances between the receivers and the transmitter are less regular than that of the setup for De Biesbosch. Their separation distances are listed in Table 4-1.

Table 5-1. Distance between transmitter and receiver.

location	distance (meter)	location	distance (meter)
1	0.5	9	7.5
2	1.8	10	8.4
3	1.9	11	9.5
4	4.0	12	10.5
5	3.5	13	2.0
6	4.0	14	5.4
7	5.5	15	9.7
8	6.1		

Two separate tests are performed in this section. The first test has the transmitting antenna directed perpendicularly to the length of the train compartment. The second test has the transmitting antenna oriented in parallel direction. The four combinations of antenna orientations are shown in Figure 5-4.a. The first test is performed with orientation 1 and 2. The second test is performed with orientation 3 and 4. The two tests generate a total of four sets of data (two sets per test and one set per antenna orientation). The locations of the receivers are reshuffled after the first test. This helps in identifying inconsistency of data caused by different hardware realizations or even malfunctioning nodes. If nodes were not reshuffled, problems caused by faulty nodes (e.g. node 9 of De Biesbosch) might remain unnoticed. This could lead to wrong conclusions. The faulty node at 9 meter in Chapter 4 was picked out because its values differ too much from its neighboring nodes. However, this dependency on neighboring nodes is not expected in train compartments. One way in detecting faulty nodes in this environment is by means of reshuffling. A faulty node which shows extreme reading at one location is very likely to show extreme readings at another location as well.

5.2.2 Data Analysis

Two nodes unexpectedly failed during the two tests, one during each test. The failed nodes were located at location 4 and 12. Data from these locations were discarded because they only represent three orientations, instead of four. The data from the remaining 13 locations are visualized in plots. Each plot visualizes data from two separate tests, as mentioned in the previous section. The plots of a selected number of locations are depicted in Figure 5-4 and Figure 5-5. The rows are ordered by the distance between the transmitter and the locations. Each row of plots represents data from a single location. The first column illustrates the relation between packet RSSI values and the sender's transmission output power. The second column illustrates the relation between the number of received preamble bytes and transmission output power. And finally, the third column illustrates the relation between packet reception rate and transmission output power.

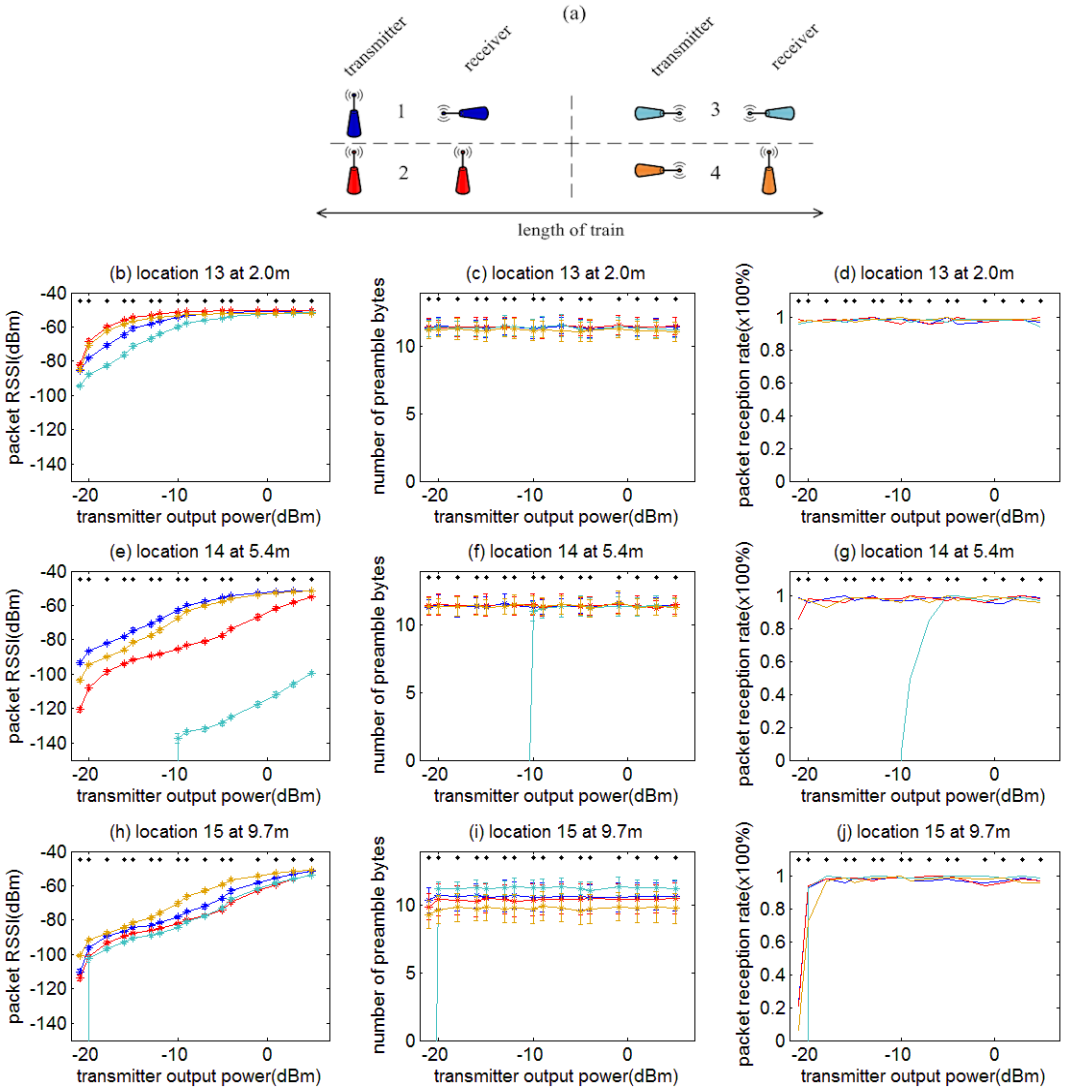

Figure 5-4. (a) Four different orientations of transmitter and receiver. (b-j) Data collected from receivers located on the ceiling. The color of the lines corresponds to the color of the orientation in (a). Column 1: signal strength of received packets. Column 2: number of received preamble bytes. Column 3: PRR.

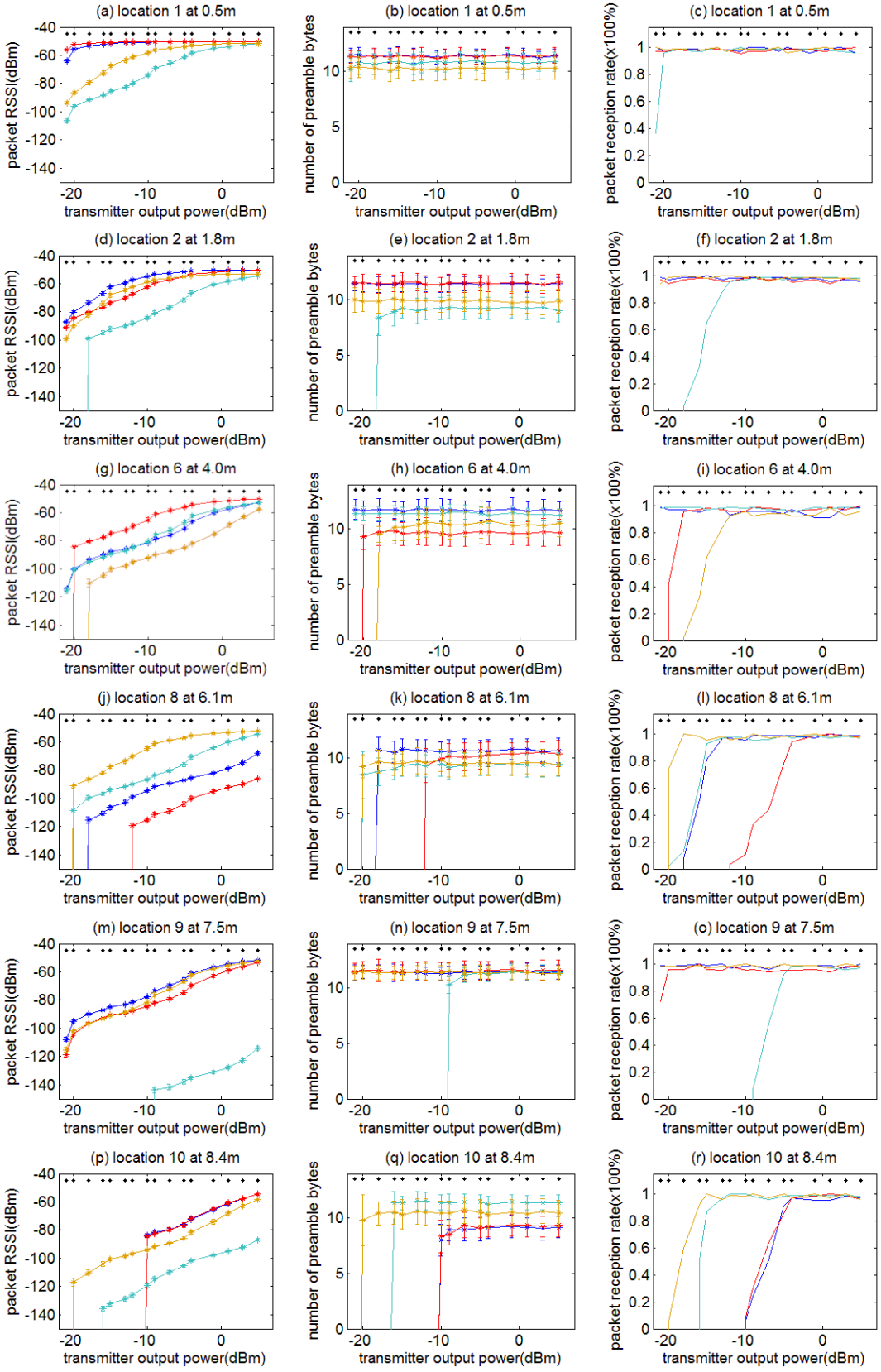

Figure 5-5. Data collected from nodes located underneath the seats. Column 1: signal strength of received packets. Column 2: number of received preamble bytes. Column 3: PRR.

Each colored line corresponds to a specific antenna orientation for the transmitter and receiver. The four different antenna orientations are depicted in Figure 5-4.a, with an unique color per orientation. The black dots on top of each plot refer to the transmission output powers of the transmitter. Figure 5-4 and Figure 5-5 visualize data from nodes located on the ceiling and underneath seats, respectively. Data from a total of 9 out of the 13 locations are illustrated by these two figures.

The first column of Figure 5-4 and Figure 5-5 show that antenna orientation does affect radio wave propagation, which contradicts the assumption made in the antenna angle experiment of Chapter 4Antenna Angle. For 10 out of 13 locations, it is discovered that the signal strength is weak when the transmitter's antenna and the receiver's antenna are both pointing in the length of the train compartment (orientation 3 of Figure 5-4.a). Figure 5-4 (location 13, 14, 15) and Figure 5-5 (location 1, 2, 9, 10) depict seven of the ten cases of this observation with light blue curves. These curves are located at the bottom of the bundle of curves. This implies that the signal strengths of received packets for the third antenna orientation are weaker than for the other three orientations. This orientation corresponds to the weakest possible angle of the radio pattern of a monopole antenna as shown in Figure 2-5.b.

Note that the light blue curves in the first column at location 9, 10, and 14 deviate significantly more from the main bundle of curves. The curve at location 9 (Figure 5-5.m) is generated from data collected by node 9, which already showed problems in Chapter 4. The same problems are likely to have caused the data to deviate from the main curve. However, this cannot be verified because this node failed during one of the two tests. Recall from the previous section about the methodology of this experiment, that node locations were reshuffled after the first test. Data from the first and second test help to identify erroneous readings caused by a hardware fault. Only one test was performed with node 9, thus it cannot be verified whether the deviation at location 9 is caused by a hardware issue.

The deviation of the light-blue curve in the first column at location 14 (Figure 5-4.d) is most likely caused by a hardware issue. The curve is generated by node 2. This node is also used at location 4 (recall that data from location 4 is discarded because its data is incomplete). The incomplete plot for the signal strength of received packets at location 4 is shown in Figure 5-6. The dark-blue curve in this figure is generated by node 2 for antenna orientation 1. This curve is found to also deviate significantly from the bundle of curves, which strongly suggests that the deviations at location 4 and 14 are caused by a hardware issue.

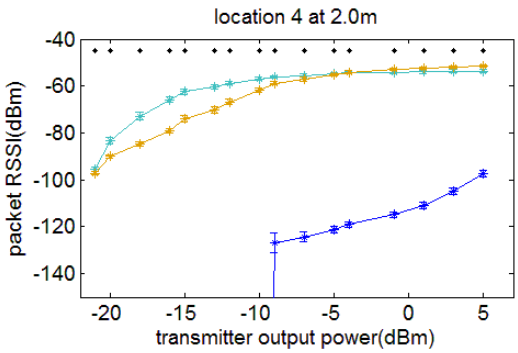

Figure 5-6. Signal strength of received packets for antenna orientation 1, 3, and 4 at location 4.

The deviation of the light-blue curve in the first column at location 10 (Figure 5-5.p) is not likely to have been caused by a hardware issue. This curve is generated by node 19, which is also used at location 1 in a separate test. The red curve of Figure 5-5.a visualizes the signal strength retrieved from node 19 at location 1 for antenna orientation 2. This curve does not deviate greatly from the bundle, as opposed to the light-blue curve at location 10. This implies that the deviation at location 10 is not caused by hardware, but rather by the environment.

The second column of Figure 5-4 and Figure 5-4 reveal not much new. The number of preamble bytes is constant over various transmission output powers as long as packets are being received. The average number of received preamble bytes for antenna orientation 1, 2, 3, and 4 are 11.3, 11.1, 10.8, and 10.6, respectively. Their standard deviation values are 0.9, 1.0, 1.1 and 1.2, respectively. The average numbers of received preamble bytes are slightly less as for De Biesbosch, which reports an average number of preamble bytes of 11.3. The standard deviations values are also larger. De Biesbosch reports a standard deviation value of 0.76 for the number of received preamble bytes. The data from the train compartments seem to favor antenna orientation 1 and 2 slightly more, where the transmitter's antenna is positioned perpendicular to the length of the train. It is possible that this is observation is contributed by the radiation pattern of the transmitter. The weakest side of the transmitter's antenna is pointed to the receivers at orientation 3 and 4. The data suggest that at least three preamble bytes are needed for train compartments, where as two preamble bytes are sufficient for De Biesbosch. This is caused by the lower average and greater standard deviation for antenna orientation 3 and 4.

The third column of Figure 5-4 and Figure 5-5 shows that results for PRR are similar to that of Chapter 4. Once the RSSI value of the packets exceeds a certain threshold, the PRRs would jump to the vicinity of 100%. The packet reception rates vary between 0% to 100% for RSSI values below this threshold. Figure 5-7 depicts the relations between RSSI values and PRR values for the four different antenna orientations of Figure 5-4.a. The thresholds for the four orientations are -76 dBm , -76 dBm, -80 dBm, and -73 dBm, respectively. Their corresponding PRR values are 91%, 85%, 91%, and 89%, respectively. These values are fairly close to each other. The plot for the third antenna orientation (Figure 5-7.c) shows that packets can still be received even for RSSI values lower than -130 dBm. This is not the case for the remaining three antenna orientations, where no packets are received at RSSI values below -130 dBm. It is unclear why antenna orientation 3 differs from the others. Figure 4-6 shows that PRR is at least 84% for RSSI values greater than -97 dBm in De Biesbosch. It also shows that PRR starts to vary wildly between 0% and 100% starting from RSSI values less than -110 dBm. Figure 5-7 shows that this point starts at values less than -80 dBm. This implies that PRR is not solely dependent on RSSI values but also on environments.

The results of this section suggest that antenna orientation exert great influences on the signal strengths of received packets. This has a direct impact on packet reception rate as shown by the plots of Figure 5-7. Signal strengths need to be high enough to achieve good PRRs. It is further inferred that reflection has less impact than antenna orientation on radio wave propagation in this environment. This is deduced from the observation that the third antenna orientation in most cases yields lower signal strengths. If reflection were to be dominant, then the order of the curves in the first column of Figure 5-4 and Figure 5-5 would have been more randomly distributed. This is not the case, as the light-blue curves of antenna orientation 3 are more often seen on

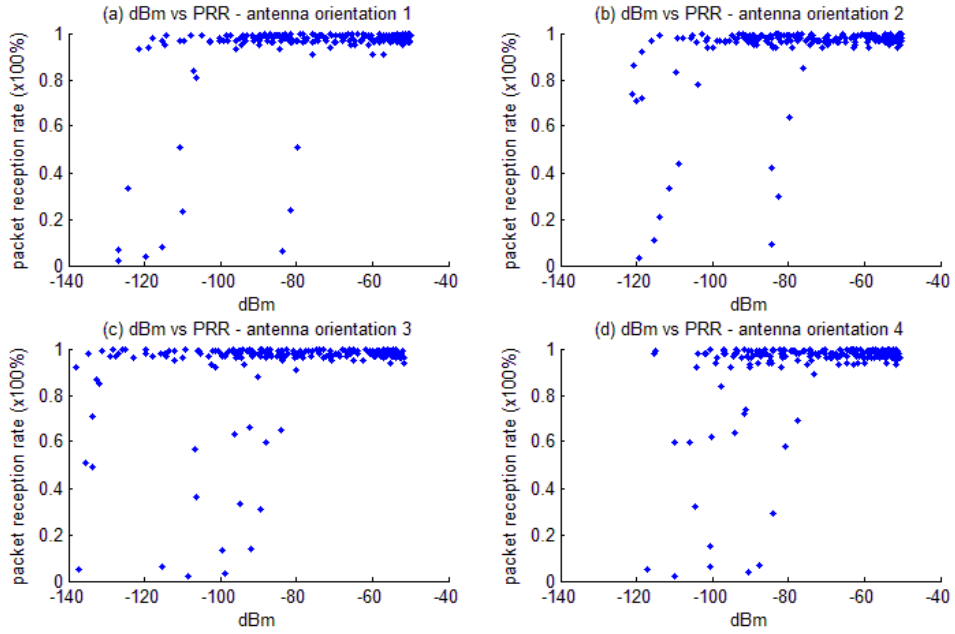

Figure 5-7. RSSI(dBm) vs. packet reception rate for the four different antenna orientations.

the bottom of the bundle of curves than elsewhere. Reflection would cause radio waves to scatter in numerous random directions regardless of antenna orientation. There was no direct evidence that this happened.

5.3 Propagation between Decks and Compartments

This section captures the characteristics of radio wave propagation in metal train compartments. It examines the propagation of radio waves between decks and between compartments.

5.3.1 Methodology

Two separate tests are carried out in this section. The antennas of all nodes, including the transmitter are directed parallel with the length of the compartment. Previous experiment showed that the received signal strengths of packets are worst in this orientation. It is believed that if a radio link can be established for this particular antenna orientation, then it is likely that radio links can also be established for other orientations. This is the reason why only this antenna orientation is considered for this experiment.

Two compartments are used in these two tests. The receiving nodes are placed in various locations throughout these two compartments. The receiving nodes were placed on the ceiling, in baggage racks, and on the side of passenger seats. For the first test, the transmitter is placed near the stairs to the decks. For the second test, the transmitter is placed on the side of a passenger seat in the lower deck. The locations of the nodes for the first and second test are shown in Figure 5-8 and Figure 5-9, respectively. The

first test focuses on the propagation between decks, whereas the second test focuses on the propagation between decks.

As in previous experiments, all receiving nodes and the transmitter remain stationary. The distances between the transmitter and receivers are irregular. Some receivers are separated from the transmitter by the ceiling between decks (e.g. location B1, B2, and B19 of Figure 5-9); others are separated by the metal sliding doors between compartments (e.g. location A27, A28, and A29 of Figure 5-8); few have line -of-sight with the transmitter (e.g. B14 of Figure 5-9).

The transmitter broadcasts packets using 16 different transmission output powers. The receivers log the packet RSSI values, the number of received preamble bytes, and the entire content of the packets. This was explained in great detail by the section on measurement setup of Chapter 4.

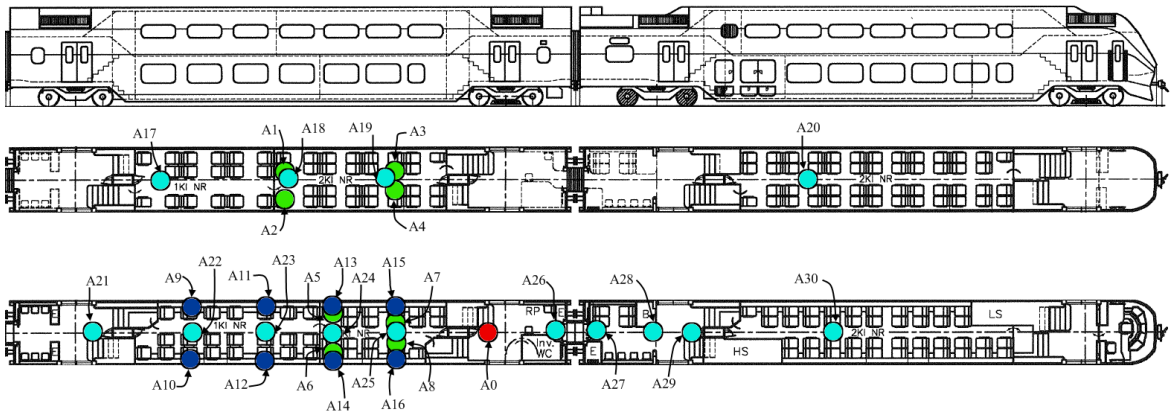

Figure 5-8. The locations of nodes for the first test. The upper deck is depicted in the middle of the figure and the lower deck is depicted in the bottom. Red: location of transmitter on the ceiling. Green: location of receiver besides the seat. Dark blue: location of receiver in the baggage rack. Light blue: location of receiver on the ceiling.

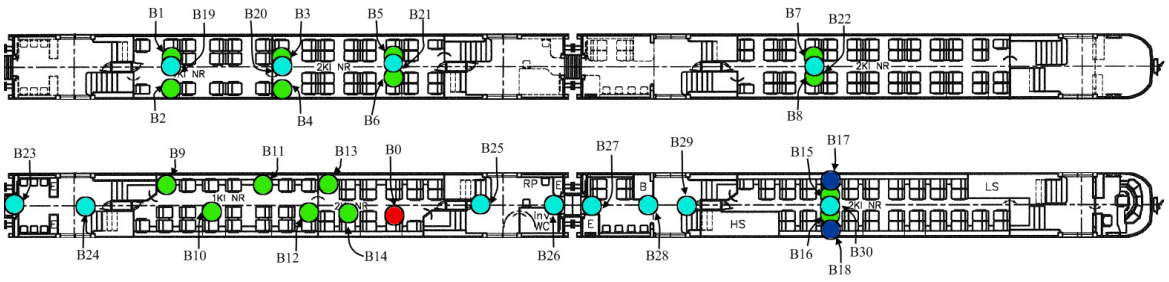

Figure 5-9. The locations of nodes for the second test. The upper deck is depicted in the top of the figure and the lower deck is depicted in the bottom. Red: location of transmitter on the ceiling. Green: location of receiver besides the seat. Dark blue: location of receiver in the baggage rack. Light blue: location of receiver on the ceiling.

5.3.2 Data Analysis

The data from location A2, A3, and A7 are discarded. The nodes at these locations fell down on the floor during the first test, because the tape gave weight. The data from location B1 and B20 are also discarded. The data on these nodes were lost, because the nodes were not properly erased before the second test was initiated.

The plots for the preambles are not shown in this section, as they do not add many new facts. The average number of received preamble bytes is 11.4 with a standard deviation of 0.7. The numbers of preamble bytes hovers around this average value whenever packets are being received. This implies that two preamble bytes are enough. However, this observation contradicts the experiment of previous section. The previous experiment on antenna directionality suggests that at least three preamble bytes are needed for the third antenna orientation.

Throughout this section, it will be apparent that the results differ from that of the previous section. This is contributed to either the close proximities of receivers or their locations. Recall that two receivers are placed within a few centimeters of each other per location underneath the seats. In the tests of this section, no nodes are placed underneath seats and no receivers are placed as close to each other as in the previous section.

Figure 5-10 and Figure 5-11 visualize data of test 1 (Figure 5-8) and test 2 (Figure 5-9). The transmitter of test 1 is placed near the entrance of the compartment. The same transmitter is placed besides a passenger seat in the lower deck for test 2. The markers and lines are colored. The blue markers refer to data collected from nodes located on the upper deck of the left train compartment, red markers refer to the lower deck of the left compartment and green markers refer to both decks of the right compartment. The colored dots on top of each plot point to the location of the receivers. The transmitter is located at distance 0. The first column depicts the relation between packet RSSI values and distance from the transmitter. The dotted colored curves represent the packet RSSI values estimated by the path loss model. Each colored curve is generated solely by the data collected from one of the three areas. The black curve shows the estimated RSSI values of the three areas combined. The corresponding path loss exponents are obtained through calculation of the minimum mean square error. The second column depicts the relation between PRR and receiver's distance. Each row of plots represents data of a particular transmission output power. These figures show only three of 16 transmission output powers: 5, -5, and -15 dBm.

Radio waves are able to propagate from one compartment to the other. This is shown by the green markers in Figure 5-10 and Figure 5-11. PRRs are in the vicinity of 100% for high transmission output powers. This does not come as a surprise, as previous experiments have shown that PRRs reach about 100% when packet RSSI values are greater than a certain threshold. Figure 5-12 illustrates this relation for test 1 (a) and test 2 (b) of the experiment in this section. For test 1, PRR is at least 88% for RSSI values greater than -111 dBm. For test 2, these two values are 87% and -103 dBm, respectively. These values resemble the results of De Biesbosch. However, they do not resemble the results of the antenna directionality experiment carried out in the train compartments.

The curves in the first column depict the estimated RSSI values of packets for a given distances. These curves are generated by taking the node closest to the transmitter of the three areas as reference nodes. The path loss exponents are deduced

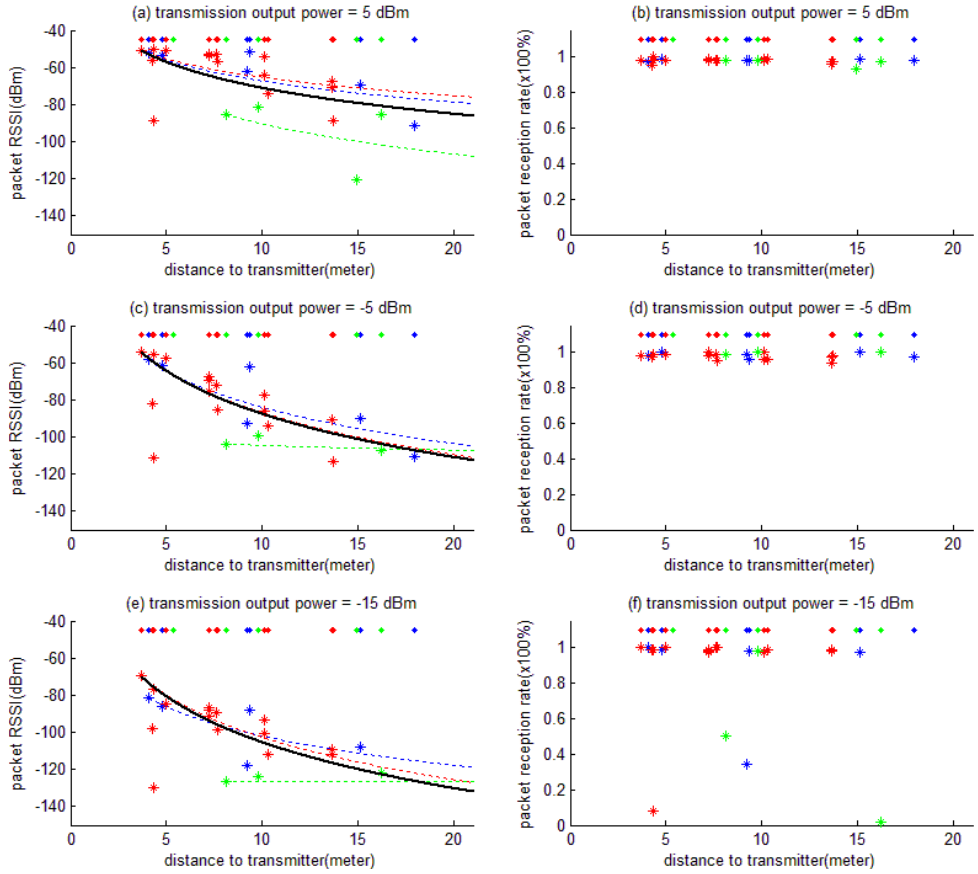

Figure 5-10. Test 1. Transmitter is located near the entrance of the compartment. Left column: packet reception rate vs. distance to the transmitter. Right Column: PRR vs. distance to the transmitter. Each color represents data retrieved from nodes in one of the three areas of the compartments.

by calculating the mean square error between observation and model. The curves represent estimations with the smallest square error. The horizontal green lines of Figure 5-10.c/e and Figure 5-11.e are generated by path loss exponents equal to zero. It shows that lack of data points results in improbable path loss exponents. An exponent of zero leads to a model where signal strength is constant over distance, meaning that no energy is lost. The complete list of path loss exponents for test 1 and test 2 of the experiment are found in Table 5-2 and Table 5-3. These tables list the path loss exponents retrieved for the three different environments and for the combination of the three environments. The number of receptive nodes per deployed nodes is listed in separate columns per area. It is possible that a deployed node is not able to receive any test packets for certain transmission output powers. A third column shows the mean square error divided by the number of receptive nodes.

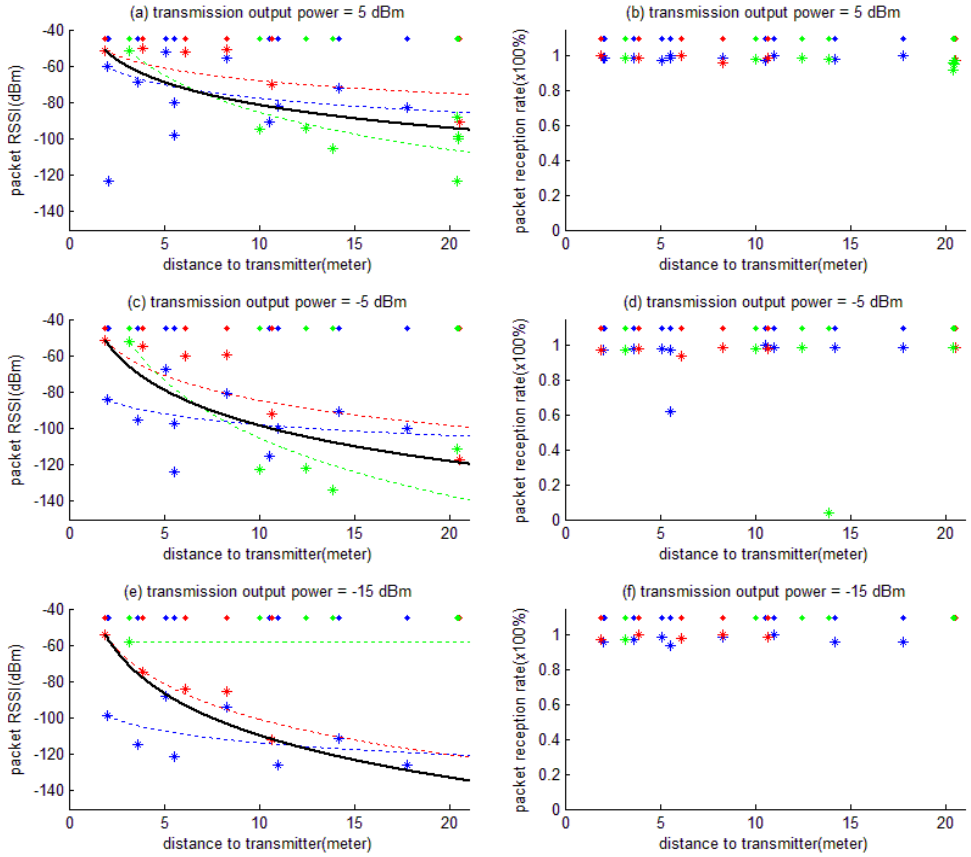

Figure 5-11. Test 2. The transmitter is located in the lower deck. Left column: packet reception rate vs. distance to the transmitter. Right Column: PRR vs. distance to the transmitter. Each color represents data retrieved from nodes in one of the three areas of the compartments.

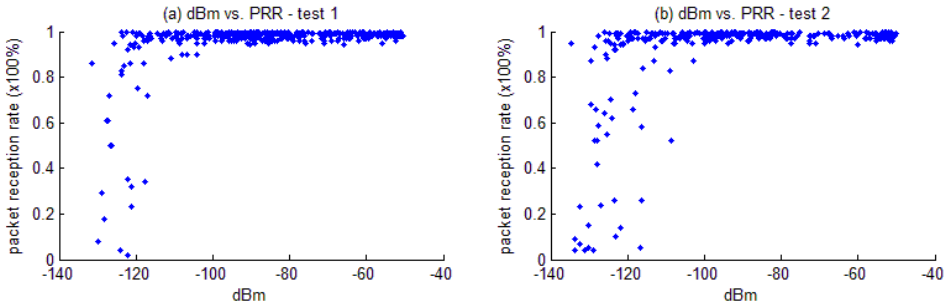

Figure 5-12. Relation between RSSI and PRR. (a) Test 1. (b) Test 2.

Table 5-2. Path loss exponents found for test 1 of the propagation experiment.

test 1												
output power (dbm)	upper deck, left compartment			lower deck, left compartment			right compartment			combined		
	PL exponent	receptive nodes / deployed nodes	MSE / receptive nodes	PL exponent	receptive nodes / deployed nodes	MSE / receptive nodes	PL exponent	receptive nodes / deployed nodes	MSE / receptive nodes	PL exponent	receptive nodes / deployed nodes	MSE / receptive nodes
< -20	2.69	3/6	4.32	8.75	9/16	32.44	n/a	0/5	n/a	8.27	12/27	50.61
-20 ~ -19	4.01	4/6	33.98	7.18	13/16	103.49	n/a	0/5	n/a	6.73	17.27	95.90
-18	3.96	4/6	31.97	6.94	14/16	72.12	n/a	0/5	n/a	6.63	18/27	70.52
-16	5.43	5/6	116.89	7.05	14/16	62.31	0.00	1/5	0.00	7.51	20/27	104.54
-15 ~ -14	5.24	5/6	95.33	7.60	15/16	254.40	0.00	3/5	8.59	8.25	23/27	250.92
-13	6.23	6/6	93.00	7.87	15/16	266.05	0.00	3/5	5.25	8.52	24/27	247.09
-12	6.47	6/6	92.16	8.04	15/16	177.48	0.00	3/5	4.67	8.68	24/27	254.27
-10	6.69	6/6	101.51	8.52	16/16	284.98	0.00	3/5	5.87	8.82	25/27	255.32
-9	6.80	6/6	101.74	8.28	16/16	282.57	0.00	3/5	9.65	8.54	25/27	248.78
-7	6.73	6/6	106.81	8.02	16/16	269.06	0.45	3/5	9.50	8.24	25/27	235.74
-5	6.52	6/6	109.61	7.54	16/16	247.62	0.83	3/5	9.13	7.75	25/27	216.88
-4 ~ -3	6.23	6/6	99.76	9.91	16/16	229.11	0.90	3/5	6.70	7.17	25/27	199.34
-1	5.69	6/6	90.77	5.90	16/16	191.64	0.30	3/5	2.77	6.30	25/27	172.65
1	5.22	6/6	80.99	1.00	16/16	171.45	0.00	3/5	2.09	5.68	25/27	158.58
3	4.51	6/6	73.61	4.35	16/16	152.53	5.80	4/5	209.87	5.59	26/27	213.89
5	3.76	6/6	76.99	3.30	16/16	131.72	5.40	4/5	191.61	4.67	26/27	202.22

Table 5-3. Path loss exponents found for test 2 of the propagation experiment.

test 2												
output power (dbm)	upper deck, left compartment			lower deck, left compartment			right compartment			combined		
	PL exponent	receptive nodes / deployed nodes	MSE / receptive nodes	PL exponent	receptive nodes / deployed nodes	MSE / receptive nodes	PL exponent	receptive nodes / deployed nodes	MSE / receptive nodes	PL exponent	receptive nodes / deployed nodes	MSE / receptive nodes
< -20	4.04	2/11	0.00	4.88	4/6	5.65	0.00	1/8	0.00	6.03	7/25	51.79
-20 ~ -19	0.32	5/11	135.94	7.01	5/6	60.85	0.00	1/8	0.00	7.76	11/25	498.38
-18	1.65	7/11	161.89	7.24	5/6	54.57	0.00	1/8	0.00	8.07	13/25	422.49
-16	2.00	8/11	153.44	6.97	5/6	47.42	0.00	1/8	0.00	8.13	14/25	423.80
-15 ~ -14	2.14	8/11	145.21	6.48	5/6	38.45	0.00	1/8	0.00	7.73	14/25	380.17
-13	2.62	9/11	153.76	6.03	5/6	36.81	0.00	1/8	0.00	7.71	15/25	354.70
-12	2.55	9/11	146.23	6.38	6/6	65.81	0.00	1/8	0.00	7.36	16/25	317.93
-10	2.27	9/11	140.53	5.81	6/6	265.43	11.05	4/8	265.43	7.28	19/25	324.43
-9	2.00	9/11	137.61	5.35	6/6	141.83	10.76	4/8	261.01	6.84	19/25	324.38
-7	2.14	10/11	201.99	5.03	6/6	169.06	10.45	4/8	248.07	6.73	20/25	388.39
-5	1.97	10/11	226.34	4.59	6/6	190.08	10.59	5/8	252.22	6.54	21/25	408.22
-4 ~ -3	1.84	10/11	234.87	4.21	6/6	197.82	9.67	6/8	212.92	6.19	22/25	376.76
-1	1.83	10/11	238.40	3.63	6/6	178.48	8.62	7/8	168.96	5.62	23/25	328.08
1	1.98	10/11	227.40	3.23	6/6	156.53	8.00	7/8	141.54	5.14	23/25	286.43
3	2.23	11/11	516.13	2.83	6/6	132.71	7.63	8/8	121.69	4.87	25/25	470.89
5	2.47	11/11	520.75	2.32	6/6	106.28	6.81	8/8	113.69	4.20	25/25	407.20

The first column of Figure 5-11 shows that communication within a deck is favored over communication between decks and between compartments. The estimated RSSI values for the lower deck (dotted red curves) are nearly always located above the other curves. The green horizontal line of Figure 5-11.e should be ignored. This line is caused because only one data point is present for this transmission output power. It is not surprising that the curves for nodes in the upper deck and in the right compartment are located lower. The receivers at these two areas have no line-of-sight with the transmitter. The radio energy was attenuated several times when the radio wave passed through obstructions.

A number of things could have made it possible for the radio wave to reach the second compartment. Note that the compartments are separated by two metal sliding doors. The radio waves could have passed through the metal structure of the compartments. Another possibility is that radio waves traveled out of the compartments through the windows and are reflected into the second compartment by the surrounding.

5.4 Discussion

The experiments in this chapter reveal that nodes can communicate with each other in metallic environments such as metal train compartments. It is shown that increased transmission power output always yields better results. Communication between two train compartments is only feasible if the sender transmits at medium to high transmission powers. High transmission power typically leads to higher packet RSSI values. It is demonstrated that RSSI values are related to PRRs.

The number of received preamble bytes is neither affected by the train environment nor by transmission output powers. The number of preamble bytes remains constant as long as packets are being received. The antenna directionality tests suggest that three bytes of preamble is sufficient. However, we doubt the validity of these tests. The compartment propagation tests suggest two preamble bytes as opposed to three. TinyOS appends by default six preamble bytes per transmission for the CC1000 transceivers. Reducing the number of preamble bytes can potentially save energy without effecting PRRs. However, this still has to be verified.

The antenna directionally experiment indicates that the characteristic of radio wave propagation is affected by antenna orientations. In particular, antennas pointing in the direction of the train yield worse results than the other three orientations. However, this is cast into doubts by the findings of the compartment propagation experiment. The tests in this experiment were performed with the same antenna orientation but results were significantly better. The deviation of the results is attributed to either the location or the close proximity of nodes. In the antenna directionality experiment, nodes were placed underneath the seats and two nodes were positioned at the same location. In the compartment propagation experiment, nodes were placed further apart from each other and they were not positioned underneath seats.

The path loss model is used to fit the data of the compartment propagation experiment. It is found that the path loss exponent value at high transmission output power for communication within decks and between decks approaches the exponent value of De Biesbosch.

This chapter falsifies the hypothesis that increased transmission output power would cause interferences. The opposite is shown to be true, as PRRs become greater for increased transmission output power.

6 Conclusion

This work explores the characteristics of radio wave propagation inside metal train compartments. It shows that wireless sensor networks can be deployed in a metallic environment such as metal train compartments. Tests have demonstrated that radio waves propagate better at higher transmission output power. This holds true for free space environments, such as De Biesbosch, but also for train compartments. Higher transmission output powers generally lead to greater signal strengths being received. Signal strength is found to relate to packet reception rate. In De Biesbosch, received signal strength above -97 dBm yields packet reception rate of at least 83.5%. In the metal train compartments, these values are -103 dBm and 87%, respectively. Packet reception rates tend to vary between 0% and 100% below these thresholds.

Tests involving preambles show that the number of received preamble bytes is neither affected by environments nor by transmission output powers. It is observed that the number of received preamble bytes remains constant as long as packet reception rate is above 0%. The transmitter precedes each test packet with 12 bytes of preambles. The receivers receive on average 11 consecutive preamble bytes. This suggests that two preamble bytes are sufficient. TinyOS sends six preamble bytes by default. Reducing the number of bytes sent will reduce power consumption. However, it is not verified in this work that two preambles is sufficient. This is left for future work.

The log-distance path loss model was used to fit the data of the experiments. It is discovered that the path loss exponent is dependent on transmission output powers. The value for the exponent decreases as the transmission output power increases. The exponent at maximum transmission output power for radio links between decks is 2.47. The exponent is 2.32 for radio links within the same deck. These values are in the same order as that for De Biesbosch, which has 2.47.

The hypothesis of the thesis states that nodes transmitting higher output power are more likely to cause interferences. This has been falsified by the results of the experiments, as they demonstrate that increased transmission output power nearly always lead to better reception.

The results of antenna directionality experiment in the train suggests that antennas pointing in the length of the compartment yield significantly worse results. The other three orientations were found to perform better. However, the results of this experiment are disputed by the results of the compartment propagation experiment. In the latter experiment, all antennas were oriented in the length of the compartments. These tests show significantly better results than any of the four orientations in the antenna directionality experiment. For now, this observation is contributed to the location of the nodes or the close proximity of receivers. Two nodes were placed at close proximity

(<10 cm) of each other at each of location. The verification of this assumption is left for future work.

We strongly encourage future researchers to carry on with this research. All experiments were done in static environments. Future tests could include the effects caused by human activities and by moving trains. During our experiments, we have encountered several cases where nodes received a stream of valid preamble bytes followed by a sync byte, while we were not transmitting. The contents mostly appear to be a random sequence of bits, however in some cases a regular pattern can be observed. We have dubbed these as *ghost packets*. Ghost packets could have been caused by natural noise or by other transmitting devices. Future work could include research on this elusive phenomenon.

Bibliography

[1] Alippi, C., & Vanini, G. (2004). Wireless sensor networks and radio localization: a metrological analysis of the MICA2 received signal strength indicator. *29th Annual IEEE International Conference on Local Computer Networks, 2004.*

[2] Arampatzis, T., Lygeros, J., & Manesis, S. (2005). A survey of applications of wireless sensors and wireless sensor networks. *Proceedings of the 2005 IEEE International Symposium on Intelligent Control*, (pp. 719-724).

[3] Buckley, J., Aherne, K., O'Flynn, B., Barton, J., Murphy, A., & O'Mathuna, C. (2006). Antenna performance measurements using wireless sensor networks. *56th Electronic Components and Technology Conference*, (pp. 1652-1657).

[4] *CC1000 single chip very low power RF transceiver*. (2007, February 7). Retrieved November 13, 2008, from Texas Instruments: http://focus.ti.com/docs/prod/folders/print/cc1000.html

[5] *CC2420 2.4 GHz IEEE 802.15.4/ZigBee-ready RF transceiver*. (2007, March 20). Retrieved November 14, 2008, from Texas Instruments: http://focus.ti.com/docs/prod/folders/print/cc2420.html

[6] Chandra, A., & Bhawan, S. (2002). Measurements of radio impulsive noise from various sources in an indoor environment at 900 MHz and 1800 MHz. *The 13th IEEE International Symposium on Personal, Indoor and Mobile Radio Communications, 2002*, *2*, pp. 639-643.

[7] Giorgetti, G., Cidronali, A., Gupta, S. K., & Manes, G. (2007). Exploiting low-cost directional antennas in 2.4 GHz IEEE 802.15.4 wireless sensor networks. *2007 European Conference on Wireless Technologies*, (pp. 217-220). Munich, Germany.

[8] Halkes, G. (2004). *Link layer phenomena in wireless sensor networks.*

[9] Hekmat, R. (2006). *Ad-hoc networks: fundamental properties and network topologies.* Dordrecht, The Netherlands: Springer.

[10] Karl, H., & Willig, A. (2005). *Protocols and architectures for wireless sensor networks.* Wiley.

[11] Kevan, T. (2006, February 1). *Shipboard machine monitoring for predictive maintenance*. Retrieved November 13, 2008, from Sensors: http://www.sensorsmag.com/sensors/article/articleDetail.jsp?id=314716

[12] Köpke, A., Swigulski, M., Wessel, K., Willkomm, D., Klein Haneveld, P. T., Parker, T. E., et al. (2008). Simultating wireless and mobile networks in OMNeT++; the mixim vision. *OMNeT Workshop 2008.*

[13] Kuorilehto, M., Kohvakka, M., Suhonen, J., Hämäläinen, P., Hännikäinen, M., & Hämäläinen, T. D. (2007). *Ultra-low energy wireless sensor networks in practice.* Wiley.

[14] Lee, S., Kim, C., & Kim, S. (2006). Constructing energy efficient wireless sensor networks by variable transmission energy level control. *The Sixth IEEE International Conference on Computer and Information Technology, 2006.*

[15] Li, X. Y., Moaveni-Nejad, K., Song, W. Z., & Wang, W. Z. (2005). Interference-aware topology control for wireless sensor networks. *Second Annual IEEE Communications Society Conference on Sensor and Ad Hoc Communications and Networks, 2005*, (pp. 263-274).

[16] Lim, L., & Wong, K. (2006). Exploring possibilities for RSS-adaptive power control in MICA2-based wireless sensor networks. *9th International Conference on Control, Automation, Robotics and Vision, 2006*, (pp. 1-6).

[17] Liu, G., Li, Z., Zhou, X., & Li, S. (2007). Transmission power control for wireless sensor networks. *International Conference on Wireless Communications, Networking and Mobile Computing, 2007 (WiCom 2007)*, (pp. 2596-2599).

[18] Puccinelli, D., & Haenggi, M. (2006). Multipath fading in wireless sensor networks: measurements and interpretation. *Proceedings of the 2006 international conference on Wireless communications and mobile computing* (pp. 1039-1044). New York: ACM.

[19] Rappaport, T. S. (2002). *Wireless Communication Princicples* (2nd ed.). Prentice Hall.

[20] Reijers, N., Halkes, G., & Langendoen, K. (2004). Link layer measurements in sensor networks. *2004 IEEE International Conference on Mobile Ad-hoc and Sensor Systems*, (pp. 224-234).

[21] *SOWNet Technologies*. (2008, November 18). Retrieved from http://www.sownet.nl

[22] Srinivasan, K., & Levis, P. (2006). RSSI is under appreciated. *Proc. of the Third Workshop on Embedded Networked Sensors (EmNets 2006).* Boston.

[23] Tanenbaum, A. S. (2002). *Computer Networks* (4th ed.). New Jersey: Pearson Education.

[24] Thelen, J., Goense, D., & Langendoen, K. (2005). Radio wave propagation in potato fields. *Proceedings of the First Workshop on Wireless Network Measurements (WiNMee 2005).* Trentino, Italy.

[25] *TinyOS*. (2008). Retrieved November 13, 2008, from http://www.tinyos.net/

[26] Van der Doorn, B., Kavelaars, W., & Langendoen, K. (2009). A protoype low-cost wakeup radio for the 868 MHz band. *The International Journal of Sensor Networks (IJSNet)* .

[27] Van Hoesel, L. F., & Havinga, P. J. (2004). A lightweight medium access protocol (LMAC) for wireless sensor networks: reducing preamble transmissions and transceiver state switches. *Proceedings of the International Conference on Networked Sensing Systems (INSS).*

[28] Wu, R. H., Lee, Y. H., Tseng, H. W., Jan, Y. G., & Chuang, M. H. (2008). Study of characteristics of RSSI signal. *IEEE International Conference on Industrial Technology, 2008*, (pp. 1-3).

[29] Ye, W., Heidemann, J., & Estrin, D. (2004). Medium access control with coordinated adaptive sleeping for wireless sensor networks. *Transition on Networking*, *13, issue 3*, pp. 493-506.

[30] Zhao, J., & Govindan, R. (2003). Understanding packet delivery performance in dense wireless sensor networks. *Proceedings of the 1st International Conference on Embedded Networked Sensor Systems*, (pp. 1-13). Los Angeles.